International Journal of Engineering Science 50 (2012) 79–100

Contents lists available at SciVerse ScienceDirect

International Journal of Engineering Science

journal homepage: www.elsevier.com/locate/ijengsci

On the longitudinal vibrations of a bar with viscous boundaries: Super-stability, super-instability, and loss of damping

Firdaus E. Udwadia *

Departments of Aerospace and Mechanical Engineering, Civil Engineering, Mathematics, and Information and Operations Management, Engineering, University of Southern California, Los Angeles, CA 90089-1453, United States

ARTICLE INFO

Article history:
Received 20 June 2011
Accepted 5 September 2011
Available online 11 October 2011

Keywords:
Longitudinal vibrations
Viscous boundary damping
Super stability
Super instability
Loss of damping
Non-discretizable continuum

ABSTRACT

This paper presents the investigation of the longitudinal motions of a bar subjected to viscous boundary conditions at each end. These viscous boundary conditions can also be thought of in terms of boundary feedback control. The system is not self-adjoint and for certain parameter regimes exhibits super-stable, super-unstable, and undamped behavior. Closed form solutions to the response of the system subjected to initial conditions and external excitation are obtained. The physical origins of the super-stable and super-unstable behavior are investigated and their intricate connectedness with the continuum model used to understand the dynamics is explained. The issue of discretization of the continuous system is discussed and it is shown that the continuum assumption bestows certain features to the response of the system that no finite dimensional approximation can qualitatively capture. Computational results corroborating the theoretical analysis are presented.

1. Introduction

This paper presents an investigation of the problem of longitudinal vibrations of a bar with viscous boundaries at each end. The boundary value problem that arises is not self adjoint. It is of special interest both from a practical as well as a pedagogical view point. Though several books illustrate this problem, the present authors have not come across any books or research papers that provide its solution. The non-self adjoint feature of the problem is what makes it interesting since it reveals special regimes of behavior that are not intuitively obvious. Furthermore, the imposed boundary conditions can also be treated as control parameters for boundary control of the bar. Such a use of boundary control of distributed parameter systems is becoming more and more important in technological applications in numerous fields ranging from the control of structural and mechanical systems to chemical and environmental process control (Balakrishnan, 2002; Barclay, Gill, & Rosen, 1998; Lions, 1971, 1988).

The problem in this paper is similar to that reported in Udwadia (2005) where a clamped bar is subjected to a viscous boundary condition at one end only. Balakrishnan (2002) was the first to point out the condition of super-stability, and Udwadia (2005) the first to consider super-instability, super-stability, and provide a complete closed form solution to the problem. A previous attempt (Hull, 1994) at the problem of a bar with a damper at one end has a non-standard treatment and provides only the response to an external excitation. The solution provided in Gürgöze and Erol (2006) appears incorrect since the authors may not have realized that the problem is not self-adjoint. In this paper we expand the solution of the problem into eigenfunctions and arrive at the solution using Laplace transforms and Green's functions. It is shown that when

* Tel.: +1 213 740 0495.
E-mail address: fudwadia@usc.edu

0020-7225/$ - see front matter © 2011 Elsevier Ltd. All rights reserved.
doi:10.1016/j.ijengsci.2011.09.001

dampers are placed at both ends of the bar the dynamics becomes much more interesting leading to complex stability regimes, and, indeed, even loss of all damping in the system.

We organize the presentation as follows. We first state the problem and then recast it as a boundary value problem to determine eigenfunctions and eigenvalues. These eigenvalues and eigenfunctions are complex because the problem is not self-adjoint. We then proceed by examining various cases to see how the spectrum of the operator is distributed. Subsequently, we determine the response in closed form via Laplace transforms using Green's functions since the eigenfunctions are not orthogonal. We then obtain the response of the system and investigate its behavior when the damping parameters lie in certain special regimes. In particular we focus our attention on the non-intuitive behavior of the system when it exhibits, super-stable, super-unstable, and undamped behavior. Using a qualitative approach, this behavior is explained by determining the coefficients of reflection at the boundaries and the impedances. Finally, we discuss discretization for the system and show that the continuum assumption bestows certain features to the response of the system that *no* finite dimensional approximation can qualitatively capture correctly.

2. Problem statement

Fig. 1 depicts a bar of linearly elastic material and uniform cross section that is attached to viscous dampers at each end. The symbols ρ, A_0 and E represent the density of the bar per unit length, the constant cross-sectional area of the bar, and its modulus of elasticity, respectively. The damping coefficients of the linear viscous dampers at each end of the bar are denoted by c_1 and c_2. The origin of the x-coordinate is attached to the left hand end of the bar, and the displacement of the bar at location x at time t is denoted by $u(x,t)$ with respect to an inertial frame of reference. The motion of the left hand end of the bar is denoted by $u(0,t) \equiv a(t)$.

The equation governing the longitudinal motion of the bar is

$$\frac{\partial^2}{\partial t^2}u(x,t) = c^2\frac{\partial^2}{\partial x^2}u(x,t) + p(x,t), \quad 0 < x < L, \tag{1}$$

with its associated boundary conditions

$$\frac{\partial}{\partial x}u(0,t) = \frac{h_1}{c}\frac{\partial}{\partial t}u(0,t) \quad \text{and} \quad \frac{\partial}{\partial x}u(L,t) = -\frac{h_2}{c}\frac{\partial}{\partial t}u(L,t) \tag{2}$$

and the given initial conditions

$$u(x,0) = f(x) + a_0 \quad \text{and} \quad \frac{\partial}{\partial t}u(x,0) = g(x) + \dot{a}_0. \tag{3}$$

Here $c^2 = \frac{E}{\rho}$, $h_1 = \frac{c_1}{EA_0}c$, and $h_2 = \frac{c_2}{EA_0}c$, where c is the wave speed along the bar. From an intuitive point of view, positive values of the dimensionless real parameter h_1 (h_2) imply that the damping in the dashpot is positive and the dashpot at the left (right) hand end of the bar causes a force that resists the motion of the bar, thereby presumably dissipating energy from the bar. One might then want to associate positive damping values with stable motions of the bar. On the other hand, negative values of $h_1(h_2)$ imply that the dashpot at the left (right) hand end of the bar has negative damping; it causes a force that abets the motion of the bar and therefore can pump energy into it. One might then want to associate negative damping values with unstable motions of the bar. We shall see in what follows that this simple intuitive picture is incomplete and that the dynamics gets interesting when the values of h_1 and h_2 have opposite signs.

The functions $f(x)$ and $g(x)$ are the given initial displacement and velocity of the bar relative to the coordinate system that is moving with the bar and attached at its left hand end. The displacement, $a_0 := a(0)$, and the velocity, $\dot{a}_0 := \dot{a}(0)$, of the left hand end of the bar at time $t = 0$ are assumed to be given, as is the force per unit length, $p(x,t)$, applied along the length of the bar. We observe that since $u(0,0) = f(0) + a(0) = a(0)$, we must have $f(0) \equiv 0$; similarly, since $\frac{\partial}{\partial t}u(0,0) = g(0) + \dot{a}(0) = \dot{a}(0)$, we must have $g(0) \equiv 0$.

3. Eigenvalues and eigenfunctions of the continuous bar

We start by assuming a solution of the form

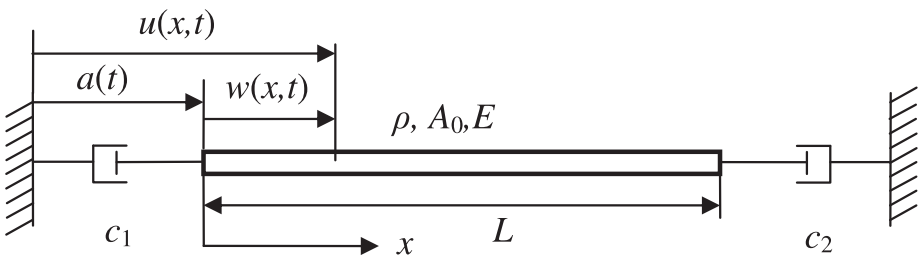

Fig. 1. A bar with two viscous boundaries.

$$u(x,t) = \varphi(x)e^{st}, \tag{4}$$

where we shall, of course, be interested only in the real part of the right-hand side of Eq. (4). Substituting this ansatz into the wave equation yields the following boundary value problem:

$$\begin{aligned} &\frac{d^2\varphi(x)}{dx^2} - \frac{s^2}{c^2}\varphi(x) = 0, \\ &\frac{d\varphi(0)}{dx} = \frac{h_1}{c}s\varphi(0), \\ &\frac{d\varphi(L)}{dx} = -\frac{h_2}{c}s\varphi(L). \end{aligned} \tag{5}$$

The general solution to the differential equation in (5) is

$$\varphi(x) = A\sinh\left(\frac{s}{c}x\right) + B\cosh\left(\frac{s}{c}x\right), \tag{6}$$

where A and B are arbitrary (complex) constants. The boundary condition at $x = 0$ reveals that either $s = 0$ or $A = h_1B$. The former imposes the rigid body eigenvalue $s_r = 0$ which has its associated eigenfunction $\phi_r = B_r = const.$ The latter yields the eigenfunction

$$\varphi(x) = B\left(\cosh\left(\frac{s}{c}x\right) + h_1\sinh\left(\frac{s}{c}x\right)\right). \tag{7}$$

Using the boundary condition at $x = L$ in (5) we obtain the eigenvalues from the relation

$$\tanh\left(\frac{sL}{c}\right) = -\frac{h_1 + h_2}{1 + h_1h_2} := -\alpha, \tag{8}$$

where we have denoted the ratio $\frac{h_1+h_2}{1+h_1h_2}$ by α. Eq. (8) can be recast in the form

$$e^{2\frac{sL}{c}} = \frac{(1-h_1)(1-h_2)}{(1+h_1)(1+h_2)} := \tilde{\alpha}, \tag{9}$$

where $\tilde{\alpha}$ is a real number. Denoting $\frac{sL}{c} = q + ip$, we obtain from (9) the relation

$$e^{2q}[\cos(2p) + i\sin(2p)] = \tilde{\alpha} \tag{10}$$

and since the right hand side is real, $\sin(2p) = 0$ which yields $2p = m\pi$, $m = 0, \pm1, \ldots$ Hence we obtain

$$e^{2q} = \pm\tilde{\alpha}, \tag{11}$$

so that when $\tilde{\alpha} > 0$

$$s_n =: \frac{c}{L}(q + ip_n) = \frac{c}{2L}\ln|\tilde{\alpha}| + i\frac{n\pi c}{L}, \quad n = 0, \pm1, \pm2, \ldots \tag{12}$$

and when $\tilde{\alpha} < 0$

$$s_n =: \frac{c}{L}(q + ip_n) = \frac{c}{2L}\ln|\tilde{\alpha}| + i\frac{(2n+1)\pi c}{2L}, \quad n = 0, \pm1, \pm2, \ldots \tag{13}$$

From Eqs. (12) and (13) we note that the real part, q, of s_n does not depend on n, and it One can summarize these results about the eigenvalues, s_n, as

$$s_n = \frac{c}{2L}\ln\left|\frac{(1-h_1)(1-h_2)}{(1+h_1)(1+h_2)}\right| + \begin{cases} \frac{c}{L}n\pi i & (|h_1| < 1 \& |h_2| < 1) \text{ or } (|h_1| > 1 \& |h_2| > 1), \\ \frac{c}{L}\frac{(2n+1)}{2}\pi i & (|h_1| < 1 \& |h_2| > 1) \text{ or } (|h_1| > 1 \& |h_2| < 1), \end{cases} \tag{14}$$

where $n = 0, \pm1, \pm2, \pm3, \ldots$ Therefore, the eigenvalues for the problem are $s_r, s_0, s_{\pm1}, s_{\pm2}, \ldots$ and the corresponding eigenfunctions are $\phi_r, \phi_0, \phi_{\pm1}, \phi_{\pm2}, \ldots$ respectively. From Eq. (14) we see that the eigenvalues, when viewed as functions of h_1 and h_2, yield the relation $s_n(h_1, h_2) = s_n(h_2, h_1)$, which is obvious from the physics of the situation, since the bar is homogeneous and isotropic. Furthermore, we observe that the damping factor for each mode

$$q(h_1, h_2) = q(h_2, h_1) = \frac{1}{2}\ln\left|\frac{(1-h_1)(1-h_2)}{(1+h_1)(1+h_2)}\right| = \frac{1}{2}\ln|\tilde{\alpha}|. \tag{15}$$

is independent of the mode number n; it is positive when $|\tilde{\alpha}| > 1$ and negative when $|\tilde{\alpha}| < 1$.

From Eq. (14) we see that when $\tilde{\alpha} \to 0$, then $q \to -\infty$, and $h_1 \to 1$ ($h_2 \neq -1$) and/or $h_2 \to 1$ ($h_1 \neq -1$). Thus for $h_1 = 1$ ($h_2 \neq -1$) and/or $h_2 = 1$ ($h_1 \neq -1$) the solution given by (1) is immediately damped out since $q = -\infty$, and the bar becomes *super-stable*. On the other hand, when $\tilde{\alpha} \to \infty$, then $q \to \infty$, and $h_1 \to -1$ ($h_2 \neq 1$) and/or $h_2 \to -1$ ($h_1 \neq 1$). The bar therefore becomes *super-unstable* when $h_1 = -1$ ($h_2 \neq 1$) and/or when $h_2 = -1$ ($h_1 \neq 1$). The behavior of the bar thus becomes interesting

and non-intuitive at these special values of h_1 (h_2) and we shall take this up when we consider the response of the bar for these special cases.

In order to better understand this behavior of the eigenvalues s_n described in (14) when $h_1, h_2 = \pm 1$, we can expand the left hand side of Eq. (8) to obtain

$$\frac{\sinh(2q) + i\sin(2p)}{\cosh(2q) + \cos(2p)} = -\alpha. \tag{16}$$

Since the right hand side of Eq. (11) is real, the imaginary part on the left-hand-side must be zero, which implies that $\sin(2p) = 0$, and $2p = m\pi$, $m = 0, \pm 1, \pm 2, \pm 3, \ldots$ Furthermore, when $m = 2n$, then $\cos(2p) = 1$, while when $m = (2n+1)$, $\cos(2p) = -1$. Using this, we can now set the real part of the left hand side of Eq. (11) to the right hand side to get

$$-\frac{\sinh(2q)}{\cosh(2q) \pm 1} = \alpha. \tag{17}$$

The plus sign in the denominator on the left hand side of Eq. (17) arises when $p_n = \{n\pi\}_{n=-\infty}^{\infty}$, and the minus sign when $p_n = \{(2n+1)\pi/2\}_{n=-\infty}^{\infty}$. For convenience we shall refer, in what follows, to these two branches of the function on the left hand side as the 'first' and the 'second' branch respectively.

The eigenvalues $s_n = c(q + ip_n)/L$ of the bar can now be determined graphically as follows. Fig. 2 shows the first and second branch of the function on the left hand side of Eq. (17) by the solid and the dashed lines respectively. For a given set of values of h_1 and h_2 the corresponding value of α is obtained; the intersection of the line α = constant with one of these branches gives the corresponding value of q. If this intersection occurs with the first branch then the imaginary part of the eigenvalues is the sequence $p_n = \{n\pi\}_{n=-\infty}^{\infty}$; if it occurs with the second branch then $p_n = \{(2n+1)\pi/2\}_{n=-\infty}^{\infty}$. We observe again that when $h_2 = 1$ and $h_1 \neq -1$, or when $h_1 = 1$ and $h_2 \neq -1$, we have $\alpha = 1$ and $q = -\infty$; and when $h_2 = -1$ and $h_1 \neq -1$, or when $h_1 = -1$ and $h_2 \neq -1$, we have $\alpha = -1$ and $q = \infty$. These situations result in the bar becoming either super-stable or super-unstable, as explained earlier.

Fig. 2 also shows, somewhat interestingly, that when $h_1 = -h_2$, $\alpha = 0$ and as seen by the intersection of the line $\alpha = 0$ with the first branch, the value of $q = 0$, with $p_n = \{n\pi\}_{n=-\infty}^{\infty}$. Thus, when $h_1 + h_2 = 0$ the bar appears to be undamped! One might intuit that this result arises because the damping of the motion produced by the dashpot at one end of the bar is exactly compensated for by the aggrandizement of the motion produced by the dashpot at the other. Somewhat less intuitive is the observation (see Eq. (8) that $\alpha \to \pm\infty$ when $h_1 = \lim_{\varepsilon \to 0}[-1/h_2 \pm \varepsilon]$. The horizontal line across the graph shown in Fig. 2 for these values of α, intersects the dashed curves again at $q = 0$, but now $p_n = \{(2n+1)\pi/2\}_{n=-\infty}^{\infty}$, since these intersections lie on the dashed curve and therefore on the so-called second branch. Hence, when $h_1 = -1/h_2$, the system again appears to have no damping!

While we have so far looked at the eigenvalues s_n of the bar for specific values of h_1 and h_2, it is informative to look at them for arbitrary values of these parameters, since they provide some non-intuitive results. Fig. 3 shows the variation of q in the $h_1 - h_2$ space. In each region we show the sign of the real part of the eigenvalue. We notice, as expected, that there are regions in this space in which $q > 0$ indicating that the system is unstable in those regions. As mentioned before, along the

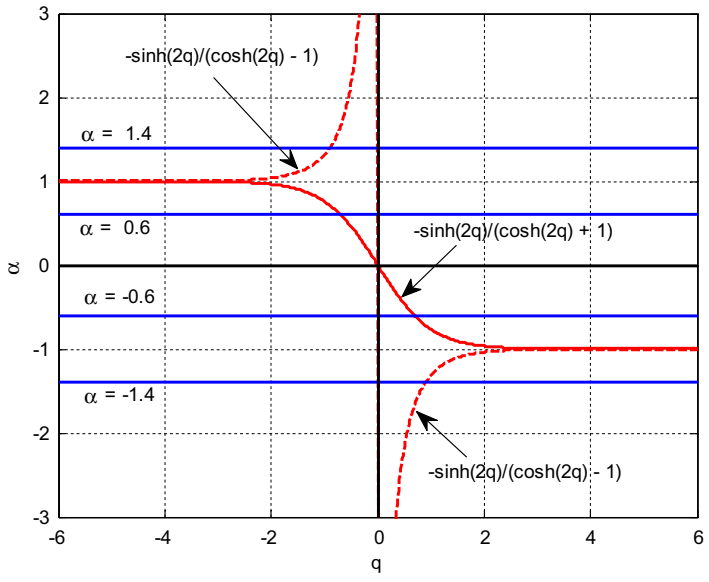

Fig. 2. The first branch (with +1 in the denominator) on the left-hand side of Eq. (17) is shown by the solid line. The second branch (with -1 in the denominator) on the left-hand side of Eq. (17) is shown by the dashed line. For a given set of values of h_1 and h_2, the corresponding value of $\alpha = (h_1 + h_2)/(1 + h_1 h_2)$, and the point of intersection of a horizontal line with this value of α and one of these branches gives the value of q. If this point of intersection falls on the first branch, $p_n = \{n\pi\}_{n=-\infty}^{\infty}$, else $p_n = \{(2n+1)\pi/2\}_{n=-\infty}^{\infty}$.

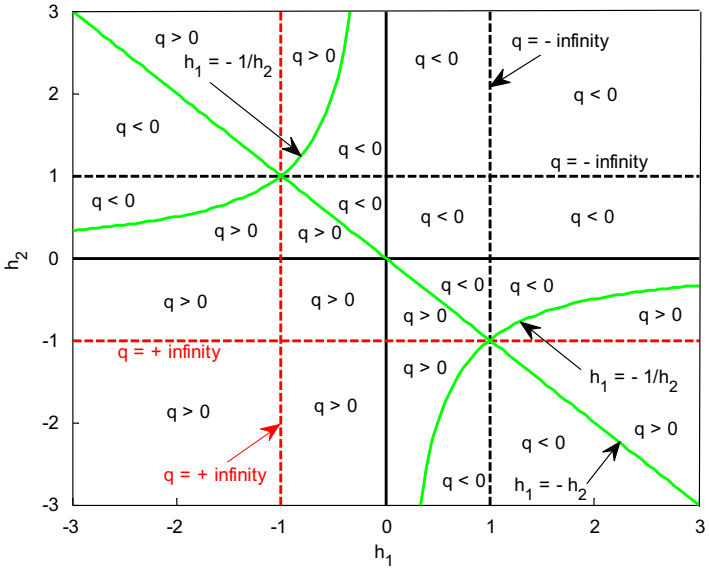

Fig. 3. Regions in the $h_1 - h_2$ space where $q < 0$ and $q > 0$. The straight line in green is the line $h_1 + h_2 = 0$, and the two curved green lines are the graph of $h_1 h_2 + 1 = 0$. Along each of these green lines $q = 0$. Along the dashed black lines $q = -\infty$, and along the dashed red lines $q = +\infty$. In regions in which $q < 0$ the system is stable; in those in which $q > 0$ the system is unstable. Note the symmetry about the line $h_1 = h_2$ (see Eq. (15)). (For interpretation of the references to colour in this figure legend, the reader is referred to the web version of this article.)

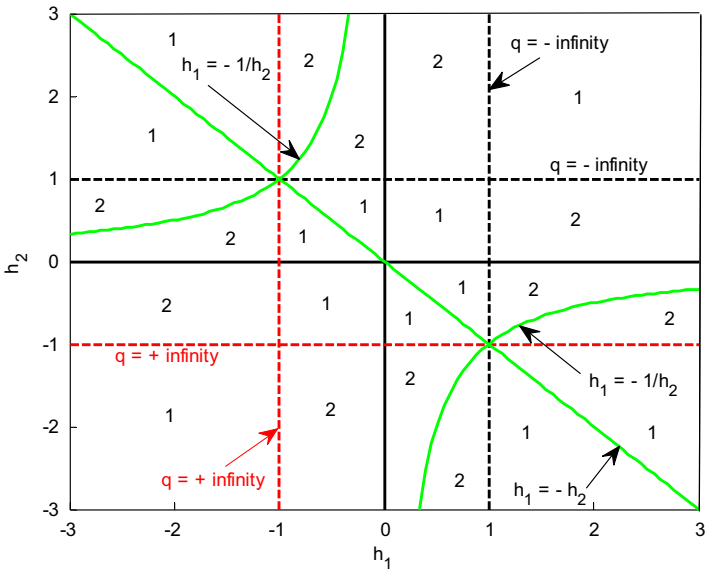

Fig. 4. Imaginary part of the eigenvalues of the system in $h_1 - h_2$ space. Each region in which $p_n = \{n\pi\}_{n=-\infty}^{\infty}$, is indicated by the numeral 1. Each region in which $p_n = \{(2n+1)\pi/2\}_{n=-\infty}^{\infty}$, is indicated by the numeral 2. Note the symmetry about the line $h_1 = h_2$.

line $h_1 = -h_2$ ($\alpha = 0$), and along the hyperbola $h_1 h_2 = -1$ ($\alpha = \pm\infty$), we have $q = 0$. These lines are shown in green in Fig. 3. The lines $h_1 = 1$ and $h_2 = 1$ (dashed black lines) form 'ridges' along which $q = -\infty$, while the lines $h_1 = -1$ and $h_2 = -1$ (dashed red lines) form 'ridges' along which $q = +\infty$. The points $(\pm 1, \pm 1)$ are clearly special points where these ridges intersect one another. Fig. 4 shows the imaginary part of the eigenvalues p_n in the different regions of the $h_1 - h_2$ space. Regions with the numeral 1 show where the sequence $p_n = \{n\pi\}_{-\infty}^{\infty}$ occurs and those with the numeral 2 show where the sequence $p_n = \{(2n+1)\pi/2\}_{-\infty}^{\infty}$ occurs. We observe that crossing the lines along which $q = 0$ (lines shown in green[1]) does not cause these sequence to change, but when the lines of 'ridges' are crossed we find that the sequences on either side of them are different.

One might intuitively interpret $h_2 < 0$ to indicate that the damping is negative, and therefore the more negative this parameter is, the more likely that the system will be unstable. However, Fig. 3 shows that this intuitive understanding of

[1] For interpretation of colour in Fig. 4, the reader is referred to the web version of this article.

the stability of the system appears incorrect. Consider first a value of $h_1 = 0.7$, which we shall keep fixed as we vary the value of h_2. For negative values of $h_2 > -0.7$ (keeping h_1 fixed at the value of 0.7), Fig. 3 shows that the system remains stable. This can be interpreted as meaning that the damping of the response of the system caused by the dashpot at the left hand end of the bar is more than compensates the response-aggrandizement created by the dashpot at its right hand end. Decreasing the value of h_2 a bit further to less than -0.7, causes the bar to become unstable as seen from the figure; this too is understandable from an intuitive standpoint for now the effect of the damping in the dashpot at the left hand end appears to have been overwhelmed by the effect of the negative damping at the right hand end. One might expect this trend to continue; however, somewhat unexpectedly, we find that for values of $h_2 < -1/0.7$ the bar becomes stable again, as seen in the figure! Next consider a value of $h_1 = 1.5$ which we shall again keep fixed as we vary the value of h_2. Applying our previous intuitive thinking we might want to infer that for all values of $h_2 > -1.5$ the system should be stable (with h_1 fixed at a value of 1.5); but instead we find that for values of $-1.5 < h_2 < -2/3$ the system becomes unstable. And even more counter-intuitively, as the figure shows, further decreases in the value of h_2 to values less than -1.5 cause the system's stability to switch back and the system becomes stable again!

Figs. 5 and 6 show 3-D plots of the q surface as a function of h_1 and h_2. Fig. 5 shows the surface along with the plane $q = 0$ (shown in green) in order to delineate the regions where the system is stable (unstable) as shown by the topography. Fig. 6 shows the topography without this plane. Regions above the plane are shown in red and yellow, those below the plane are shown in blue.

Noting Eqs. (4) and (7), the nth eigenfunction is give by

$$\begin{aligned}\varphi_n(x,t) &= 2(D_n + iC_n)\left(\cosh\left(\frac{s_n x}{c}\right) + h_1 \sinh\left(\frac{s_n x}{c}\right)\right)e^{s_n t} = (D_n + iC_n)\left\{(1+h_1)e^{\frac{x}{L}(q+ip_n)} + (1-h_1)e^{-\frac{x}{L}(q+ip_n)}\right\}e^{\frac{c}{L}(q+ip_n)t} \\ &= (D_n + iC_n)\left\{(1+h_1)e^{\frac{q}{L}(ct+x)+i\frac{p_n}{L}(x+ct)} + (1-h_1)e^{-\frac{q}{L}(x-ct)-i\frac{p_n}{L}(x-ct)}\right\}, \end{aligned} \tag{18}$$

where the eigenfrequencies, $s_n =: \frac{c}{L}(q + ip_n)$, are given by relation (14) and depend on the values of h_i, $i = 1,2$, and the number two in the first equality in Eq. (18) is used only for convenience and can be viewed as part of the arbitrary constants. Since we are only interested in the real part of the solution, the real part of the right hand side of (18) yields

$$\begin{aligned}\Re\{\varphi_n(x,t)\} = D_n &\left((1+h_1)\cos\left(\frac{p_n}{L}(x+ct)\right)e^{\frac{q}{L}(x+ct)} + (1-h_1)\cos\left(\frac{p_n}{L}(x-ct)\right)e^{-\frac{q}{L}(x-ct)}\right) \\ - C_n &\left((1+h_1)\sin\left(\frac{p_n}{L}(x+ct)\right)e^{\frac{q}{L}(x+ct)} - (1-h_1)\sin\left(\frac{p_n}{L}(x-ct)\right)e^{-\frac{q}{L}(x-ct)}\right). \end{aligned} \tag{19}$$

Relation (19) indicates that $\varphi_n(x,t)$ can be regarded as a set of exponentially damped traveling waves.

When $h_1 = 1$ and $h_2 \neq -1$, then $\alpha = 1$ and from Fig. 2 we see that $q = -\infty$. Eq. (19) then shows that our assumed solution seems to vanish, since $1 - h_1 = 0$, and the second member in each of the brackets in (19) becomes zero while the corresponding first members go to zero because of the exponential term. Similarly when $h_1 = -1$and $h_2 \neq 1$, then $\alpha = -1$ and from Fig. 2 we see that $q = \infty$; Eq. (19) then shows us that the response explodes for $t > L/c$, since now $1 + h_1 = 0$, so that the first member in each bracket on the right hand side of (19) is zero, while the exponential terms in the second members of each bracket cause the response to go to infinity. Also since q is a symmetric function of h_1 and h_2 (see Eq. (15)) one can interchange the

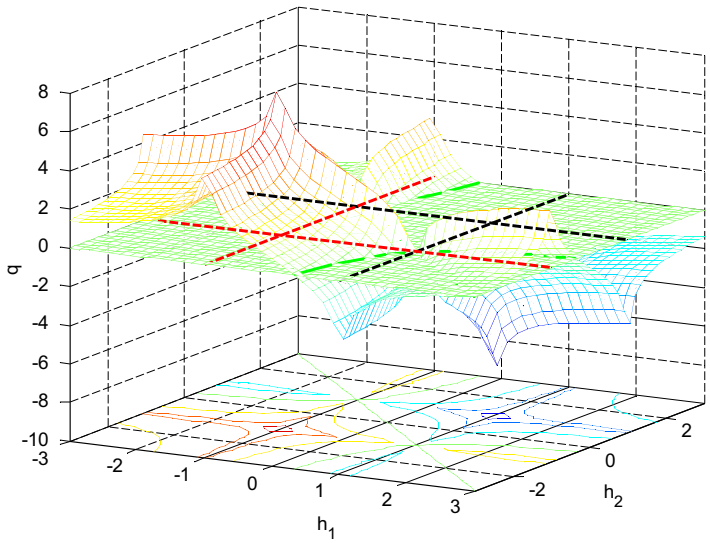

Fig. 5. Three dimensional plot of q versus h_1 and h_2. The green surface is the plane $q = 0$.Values of $q < 0$ are shown below this surface, and are plotted in blue; values of $q > 0$ are shown in red. The dashed black lines are ridges along which $q = -\infty$ and the dashed red lines are ridges along which $q = +\infty$. The ridges have been shown to be of finite height in order to see the structure of the rest of the surface. (For interpretation of the references to colour in this figure legend, the reader is referred to the web version of this article.)

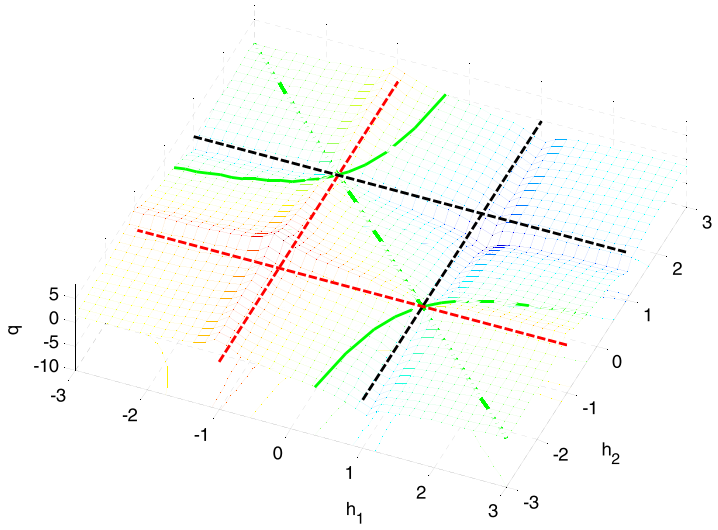

Fig. 6. Three dimensional plot of q versus h_1 and h_2 without the surface $q = 0$ showing the complex structure of the surface that dictates stability of the system.

roles of h_1 and h_2 in the previous statements as far as the stability of the system goes. Thus when $h_2 = 1$ and $h_1 \neq -1$, then $\alpha = 1$ and $q = -\infty$, so that the response goes to zero instantly; similarly when $h_2 = -1$ and $h_1 \neq 1$, then $\alpha = -1$ and $q = \infty$ so that the response becomes unbounded for $t > L/c$. We shall see that these two types of responses warrant labeling the behavior of the bar as super-stable and super-unstable, respectively.

4. Determination of the vibratory response

As was pointed out above, our boundary value problem is not self-adjoint and a direct approach by using eigenfunctions needs to be done with considerable care since they are not orthogonal, and may not span the entire space. Therefore, we proceed by using more general methods. We take the Laplace transform of Eqs. (1)–(3) with respect to time to obtain

$$\frac{d^2U(x,s)}{dx^2} - \frac{s^2}{c^2}U(x,s) = -\frac{sf(x) + sa_0 + g(x) + \dot{a}_0 + P(x,s)}{c^2}, \tag{20}$$
$$\frac{dU(0,s)}{dx} = \frac{h_1}{c}sU(0,s) - \frac{h_1}{c}a_0,$$
$$\frac{dU(L,s)}{dx} = -\frac{h_2}{c}sU(L,s) + \frac{h_2}{c}(f(L) + a_0),$$

where we have denoted the Laplace transform of $u(x,t)$ by $U(x,s)$, and of $p(x,t)$ by $P(x,s)$.

In order to simplify the problem, we use the substitution

$$U(x,s) = V(x,s) + \frac{a_0}{s}, \tag{21}$$

which causes the equation set (20) to simplify to

$$\frac{d^2V(x,s)}{dx^2} - \frac{s^2}{c^2}V(x,s) = -\frac{sf(x) + g(x) + \dot{a}(0) + P(x,s)}{c^2} := -\frac{\Gamma(x,s)}{c^2}, \tag{22}$$
$$\frac{dV(0,s)}{dx} = \frac{h_1}{c}sV(0,s), \tag{23}$$
$$\frac{dV(L,s)}{dx} = -\frac{h_2}{c}sV(L,s) + \frac{h_2}{c}f(L). \tag{24}$$

We can now think of the right hand sides of the three equations (22)–(24) as the 'data' for our two point boundary value problem (BVP). Since the problem is linear, this data can be split into two data sets, each set comprising the data for a separate independent BVP, whose individual solutions will be easier to handle. Thus we split the original data set given by Eqs. (22)–(24) into the following two sets as follows

$$\left\{-\frac{\Gamma(x,s)}{c^2};\ \frac{h_1}{c}sV(0,s),\ -\frac{h_2}{c}sV(L,s) + \frac{h_2}{c}f(L)\right\} = \left\{-\frac{\Gamma(x,s)}{c^2};\ \frac{h_1}{c}sV(0,s),\ -\frac{h_2}{c}sV(L,s)\right\}$$
$$+ \left\{0;\ \frac{h_1}{c}sV(0,s),\ -\frac{h_2}{c}sV(L,s) + \frac{h_2}{c}f(L)\right\}. \tag{25}$$

The brackets on the right give the data for each of the two BVPs, which are solved separately. We then add the individual solutions of these two BVPs to obtain the final response. We define $f(x)$ and $g(x)$ to be zero outside of the interval $(0,L)$.

We shall denote the solution to the BVP using the first data set on the right hand side of (25) by $V_1(x,s)$, and the solution to the BVP with the second set data set by $V_2(x,s)$. The solution of the BVP described by Eqs. (22)–(24) can then be written as

$$V(x,s) = V_1(x,s) + V_2(x,s). \tag{26}$$

To obtain $V_1(x,s)$, we use the Green's function approach. The Green's function is the solution to our two-point BVP that uses the data set $\left\{\delta(x-\xi);\ \frac{h_1}{c}sV_1(0,s),\ -\frac{h_2}{c}sV_1(L,s)\right\}$. Appendix A.1, shows that the Green's function is

$$G(x,\xi;s) = \begin{cases} G_l(x,\xi;s) = \frac{c\left(\sinh\left(\frac{s\xi}{c}\right)\gamma_1(s) - \cosh\left(\frac{s\xi}{c}\right)\gamma_2(s)\right)\varphi(x,s)}{s\Delta(s)} & 0 \leqslant x < \xi \leqslant L, \\ G_r(x,\xi;s) = \frac{c\left(\sinh\left(\frac{sx}{c}\right)\gamma_1(s) - \cosh\left(\frac{sx}{c}\right)\gamma_2(s)\right)\varphi(\xi,s)}{s\Delta(s)} & 0 \leqslant \xi < x \leqslant L, \end{cases} \tag{27}$$

where we have denoted

$$\varphi(x,s) = \cosh\left(\frac{s}{c}x\right) + h_1 \sinh\left(\frac{s}{c}x\right), \tag{28}$$

$$\gamma_1(s) = \sinh\left(\frac{sL}{c}\right) + h_2 \cosh\left(\frac{sL}{c}\right), \tag{29}$$

$$\gamma_2(s) = \cosh\left(\frac{sL}{c}\right) + h_2 \sinh\left(\frac{sL}{c}\right) \tag{30}$$

and

$$\Delta(s) = \gamma_1(s) + h_1\gamma_2(s). \tag{31}$$

The solution $V_1(x,s)$ can now be written as

$$V_1(x,s) = -\frac{1}{c^2}\int_0^x G_r(x,\xi;s)\Gamma(\xi,s)d\xi - \frac{1}{c^2}\int_x^L G_l(x,\xi;s)\Gamma(\xi,s)d\xi. \tag{32}$$

It can be verified that the Green's function has poles at $s = 0$, and $s = s_n$ which are exactly the eigenvalues previously obtained in Eq. (8). The latter poles are obtained by setting $\Delta(s)$ to zero, which yields an equation that is exactly the same as Eq. (8) (or (9)). The poles s_n are all therefore seen to be simple and are explicitly given by relation (14); they are dependent, as we saw in Section 3, on the parameters h_1 and h_2. The eigenfunctions corresponding to these poles are given by $\varphi_n(x) := \varphi(x,s_n)$, where $\varphi(x,s)$ is given in Eq. (28).

The solution, $V_2(x,s)$, to the BVP with the second set of data on the right hand side of relation (25) is very simple to obtain, as shown in Appendix A.2. It is simply

$$V_2(x,s) = \frac{h_2 f(L)}{s\Delta(s)}\varphi(x,s). \tag{33}$$

The solution to our original BVP described in Eq. (20) is then given by

$$U(x,s) = V_1(x,s) + \frac{a_0}{s} + V_2(x,s) = -\frac{1}{c^2}\int_0^x G_r(x,\xi,s)\Gamma(\xi,s)d\xi - \frac{1}{c^2}\int_x^L G_l(x,\xi,s)\Gamma(\xi,s)d\xi + \frac{a_0}{s} + f(L)\frac{h_2}{s\Delta(s)}\varphi(x,s), \tag{34}$$

where

$$\Gamma(x,s) = sf(x) + g(x) + \dot{a}_0 + P(x,s). \tag{35}$$

Appendix A.3, shows that the inverse Laplace transform of the Green's function is given by

$$L^{-1}\{G_{l,r}(x,\xi,s)\} = -\frac{c}{(h_1+h_2)} - \frac{c^2}{(1-h_1^2)L}\sum_{n=-\infty}^{\infty}\frac{1}{s_n}e^{s_n t}\varphi_n(x)\varphi_n(\xi) \tag{36}$$

and that (see Appendix A.3)

$$L^{-1}\{sG_{l,r}(x,\xi,s)\} = -\frac{c^2}{(1-h_1^2)L}\sum_{n=-\infty}^{\infty}e^{s_n t}\varphi_n(x)\varphi_n(\xi), \tag{37}$$

where s_n is given in Eq. (14). We also note that (see Appendix A.4)

$$L^{-1}\left\{f(L)\frac{h_2}{s\Delta(s)}\varphi(x,s)\right\} = f(L)\frac{h_2}{h_1+h_2} + f(L)\frac{h_2 c}{(1-h_1^2)L}\sum_{n=-\infty}^{\infty}\frac{\varphi_n(x)e^{s_n t}}{s_n\gamma_2(s_n)}. \tag{38}$$

Using relations (36)–(38) and taking the inverse Laplace transform on both sides of Eq. (34) we now obtain the closed form expression for the response of the system as

$$u(x,t) = \left[a_0 + \dot{a}_0 \frac{L}{c(h_1+h_2)} + \frac{1}{c(h_1+h_2)} \int_0^L g(\xi)d\xi + f(L)\frac{h_2}{(h_1+h_2)}\right] + \frac{1}{(1-h_1^2)L} \sum_{n=-\infty}^{\infty} \varphi_n(x) e^{s_n t}$$
$$\times \int_0^L \varphi_n(\xi)\left[f(\xi) + \frac{g(\xi)+\dot{a}_0}{s_n}\right]d\xi + \frac{1}{c(h_1+h_2)} \int_0^t \int_0^L p(\xi,\tau)d\xi d\tau + \frac{1}{(1-h_1^2)L} \sum_{n=-\infty}^{\infty} \frac{1}{s_n}\varphi_n(x)$$
$$\times \int_0^t e^{s_n(t-\tau)}\left[\int_0^L \varphi_n(\xi)p(\xi,\tau)]d\xi\right]d\tau + f(L)\frac{h_2 c}{(1-h_1^2)L} \sum_{n=-\infty}^{\infty} \frac{\varphi_n(L)\varphi_n(x)e^{s_n t}}{s_n}, \quad h_1+h_2 \neq 0,\ h_1 \neq \pm 1,\ \forall n. \tag{39}$$

We see from Eq. (39) that the total response of the vibrating bar can be thought of as consisting of: (a) a static displacement indicated by the first line on the right hand side of Eq. (39); (b) a vibratory response caused by the initial conditions indicated in the second line on the right hand side; (c) a vibratory response generated by the excitation $p(x,t)$ indicated on the third line; (d) and a vibratory response contribution from the initial displacement condition at the right hand end of the bar shown in the last line.

When $p(x,t) = p_1(x)p_2(t)$, the third line on the right hand side of Eq. (39) further simplifies to

$$\frac{1}{c(h_1+h_2)} \int_0^L p_1(\xi)d\xi \int_0^t p_2(\tau)d\xi + \frac{1}{(1-h_1^2)} \sum_{n=-\infty}^{\infty} \frac{1}{s_n}\varphi_n(x)\left[\int_0^L \varphi_n(\xi)p_1(\xi)d\xi\right] \int_0^t e^{s_n(t-\tau)}p_2(\tau)d\tau. \tag{40}$$

5. Response of the system for special values of h_1 and h_2

We consider the response of the system in this section for special values of the parameters when the system exhibits super-stable, super-unstable, and undamped behavior.

5.1. Response of the system for special values $h_1 \neq -1$, $h_2 = 1$

In this sub-section we investigate the Green's function when $h_1 = \pm 1$ and $h_2 = \pm 1$. We show that for these values of damping the behavior of the bar becomes non-intuitive and interesting. When $h_2 = 1$, from Eqs. (29) and (30) we see that $\gamma_1(s) = \gamma_2(s)$. Thus, for $h_1 \neq -1$ and $\gamma_1(s) \neq 0$ Eq. (27) reduces to the following Green's function

$$G(x,\xi;s) = \begin{cases} G_l(x,\xi;s) = \frac{c\left(\sinh\left(\frac{s\xi}{c}\right) - \cosh\left(\frac{s\xi}{c}\right)\right)\phi(s,x)}{s(1+h_1)} & 0 \leqslant x < \xi \leqslant L, \\ G_r(x,\xi;s) = \frac{c\left(\sinh\left(\frac{sx}{c}\right) - \cosh\left(\frac{sx}{c}\right)\right)\phi(s,\xi)}{s(1+h_1)} & 0 \leqslant \xi < x \leqslant L. \end{cases} \tag{41}$$

We note, somewhat surprisingly, that *all* the poles in the Green's function have now disappeared except the one at $s = 0$! Using this Green's function in Eq. (41) the response can be written as

$$U(x,s) = \int_0^x \frac{1}{2sc} e^{-\frac{s(x-\xi)}{c}}\Gamma(\xi,s)d\xi + \int_x^L \frac{1}{2sc} e^{-\frac{s(\xi-x)}{c}}\Gamma(\xi,s)d\xi + \eta_1 \int_0^L \frac{1}{2cs} e^{-\frac{s(\xi+x)}{c}}\Gamma(\xi,s)d\xi + \frac{a_0}{s} + f(L)$$
$$\times \frac{\left[e^{-\frac{s(L-x)}{c}} + \eta_1 e^{-\frac{s(L+x)}{c}}\right]}{2s}, \tag{42}$$

where we have denoted the reflection coefficient $\eta_1 := \frac{(1-h_1)}{(1+h_1)}$. Furthermore, from Eq. (41) we also find that $\lim_{s\to 0} sG_l(x,\xi,s) = \lim_{s\to 0} sG_r(x,\xi,s) = -c/(1+h_1)$, and noting the expression for Γ given in (35), we obtain by using (34) with $h_2 = 1$,

$$\lim_{t\to\infty} u(x,t) = \lim_{s\to 0} sU(x,s) = \lim_{s\to 0} \frac{1}{c(1+h_1)} \int_0^L [sf(\xi) + g(\xi) + \dot{a}_0 + P(\xi,s)]d\xi + a_0 + f(L)\lim_{s\to 0}\frac{\varphi(x,s)}{\Delta(s)}$$
$$= a_0 + f(L)\frac{1}{1+h_1} + \frac{\dot{a}_0 L}{c(1+h_1)} + \frac{1}{c(1+h_1)} \int_0^L [g(x) + P(x,0)]dx, \tag{43}$$

thereby obtaining the long-time response of the system. Later, we shall further refine our understanding of this long term response by looking at the response of the vibratory system, which we next determine.

Since $f(x)$ and $g(x)$ are defined to be zero outside the interval $(0,L)$, the inverse Laplace transform of Eq. (42), is given by

$$u(x,t) = a_0 + \frac{1}{2}f(x-ct) + \frac{1}{2}f(x+ct) + \frac{\eta_1}{2}f(ct-x) + \frac{f(L)}{2}\left[H\left(t - \frac{L-x}{c}\right) + \eta_1 H\left(t - \frac{L+x}{c}\right)\right]$$
$$+ \begin{cases} \frac{\dot{a}_0}{2}t, & \text{for } 0 < t < \frac{x}{c} \\ \frac{\dot{a}_0}{2}\frac{x}{c}, & \frac{x}{c} \leqslant t \end{cases} + \begin{cases} \frac{\dot{a}_0}{2}t, & \text{for } 0 \leqslant t < \frac{L-x}{c} \\ \frac{\dot{a}_0}{2}\frac{L-x}{c}, & \frac{L-x}{c} \leqslant t \end{cases} + \begin{cases} \frac{\eta_1\dot{a}_0}{2}(t-\frac{x}{c}), & \text{for } \frac{x}{c} \leqslant t < \frac{x+L}{c} \\ \frac{\eta_1\dot{a}_0}{2}\frac{L}{c}, & \frac{x+L}{c} \leqslant t \\ 0, & \frac{x}{c} > t \end{cases}$$
$$+ \frac{1}{2}\int_0^t g(x-c\tau)d\tau + \frac{1}{2}\int_0^t g(x+c\tau)d\tau + \frac{1}{2}\eta_1 \int_0^t g(c\tau-x)d\tau + \frac{1}{2c}\int_0^x \int_0^{t-\frac{x-\xi}{c}} p(\xi,\tau)d\tau d\xi$$
$$+ \frac{1}{2c}\int_x^L \int_0^{t-\frac{\xi-x}{c}} p(\xi,\tau)d\tau d\xi + \frac{\eta_1}{2c}\int_0^L \int_0^{t-\frac{\xi+x}{c}} p(\xi,\tau)d\tau d\xi. \tag{44}$$

Here $H(t)$ is the unit step function and the terms involving the factor η_1 represent reflections from the left end of the boundary with a reflection coefficient η_1. The first line on the right hand side of equation represents the response caused by of the initial displacement (a_0 and $f(x)$), the second and third lines represent the response due to the initial velocity ($\dot{a}_0$ and $g(x)$), and the fourth line shows the effect of the external excitation ($p(x,t)$). It is important to note the *absence* of any eigenfunctions in the solution; no standing waves are generated, and the solution shows no s0-called modeshapes of vibration!

It is interesting to look at the response of the system when the external excitation is absent. Eq. (44) indicates that the response consists of the traveling waves reflected from the left boundary. We next determine at what instant of time these waves stop making contributions to the vibratory displacement of the bar.

The effect of the initial displacement (a_0 and $f(x)$) as shown in the first line on the right in Eq. (44). The response shows a permanent displacement a_0, and a vibratory effect caused by the initial displacement $f(x)$. Consider any point on the bar located at x_0 and its displacement in time caused by $f(x)$. Since $f(x) \neq 0$ only for $0 \leqslant x \leqslant L$, as time increases from zero the argument $x_0 - ct$ of $f(x_0 - ct)$ will constantly decrease and there will come a time beyond which the term $f(x_0 - ct)/2$ will make no contribution to the vibratory response of the system; this time will be $t_1 = x_0/c$. The times for the other two terms, $f(x_0 + ct)/2$ and $f(ct - x_0)/2$, when they stop contributing to the vibratory response will similarly be $t_2 = (L - x_0)/c$ and $t_3 = (L + x_0)/c$ respectively. Thus, the time after which the terms $f(x_0 - ct)/2$, $f(x_0 + ct)/2$, $f(ct - x_0)/2$ will make no vibratory contributions to the displacement at the point x_0 is $t_{\max,x_0} = \max(t_1, t_2, t_3) = (L + x_0)/c$. Moreover the last member (containing $f(L)$) on the first line of (44) shows that for $t > 2L/c$ the contribution to the response of that member is simply a permanent displacement $f(L)/(1 + h_1)$. We therefore find that after time $t_{\max} = 2L/c$ no point of the bar is caused to vibrate because of the initial displacement $f(x)$. Furthermore, the point at the right end boundary of the bar will be the last one to 'feel' the vibratory consequence of the presence of the initial displacement $f(x)$. The initial displacement (a_0 and $f(x)$) thus results simply in a permanent displacement of the system of $a_0 + f(L)/(1 + h_1)$ beyond time $t > 2L/c$.

We next look at the effect of the initial velocity $(\dot{a}_0, g(x))$ on the response of the system as given by the second and third lines on the right of Eq. (44). We observe that while the initial displacement a_0 causes only a permanent displacement of the system, the initial velocity $\dot{a}_0$ generates a vibratory response as does the term $g(x)$. The response caused by g (x) at time $t \geqslant \max[x_0/c, (L - x_0)/c]$ at the location $x = x_0$ is given by

$$\frac{1}{2}\int_0^{\frac{2L}{c}} g(x_0 - c\tau)d\tau + \frac{1}{2}\int_0^{\frac{2L}{c}} g(x_0 + c\tau)d\tau + \frac{1}{2}\eta_1 \int_0^{\frac{2L}{c}} g(x_0 + c\tau)d\tau$$
$$= \frac{1}{2c}\int_0^{x_0} g(\eta)d\eta + \frac{1}{2c}\int_{x_0}^{L} g(\eta)d\eta + \frac{1}{2c}\eta_1 \int_0^{L} g(\eta)d\eta = \frac{1}{c(1+h_1)}\int_0^{L} g(\eta)d\eta, \tag{45}$$

which we notice is a constant in time and does not depend on the location x_0 along the bar. Specifically, when $t > L/c$ this response that is given by the right hand side of relation (45) for *every* point on the bar.

Also, for all time $t > 2L/c$ the displacement $\frac{\dot{a}_0 L}{c(1+h_1)}$ due to $\dot{a}_0$ is obtained from the second line of Eq. (44).

Consequently, in the absence of external excitation, a further refinement of Eq. (43) is given by

$$u(x,t) = a_0 + f(L)\frac{1}{(1+h_1)} + \frac{1}{c(1+h_1)}\dot{a}_0 L + \frac{1}{c(1+h_1)}\int_0^L g(x)dx \quad \text{for all} \quad t > \frac{2L}{c}. \tag{46}$$

Therefore in the absence of external excitation, after a time $2L/c$ every point of the *bar has a constant displacement; the bar comes to rest in finite time*. The bar is super-stable and beyond a time $t = 2L/c$ it is at rest. Interestingly enough, the initial displacement given to the bar affects its final displacement only through the term containing $f(L)$.

In the special case when $h_1 = h_2 = 1$, we find that $\eta_1 = 0$, and the magnitude of the long-term displacement of the system caused by the initial conditions can be simply obtaining by substituting $h_1 = 1$ in Eq. (46). However, as seen from Eq. (44) this static displacement now ensues for all $t > L/c$. Thus, beyond a time $t = L/c$ the bar is at rest; it is superstable.

5.2. Response of the system for the special values $h_2 = -h_1$

In this sub-section we look at the case when $h_1 = -h_2 \neq 1$. We note that the expressions in Eq. (39) are not valid when $h_1 + h_2 = 0$. The Green's function involved in the solution $V_1(x,s)$ now becomes

$$G(x,\xi;s) = \begin{cases} G_l(x,\xi;s) = \frac{c\left(\gamma_1(s)\sinh\left(\frac{s\xi}{c}\right) - \gamma_2(s)\cosh\left(\frac{s\xi}{c}\right)\right)\varphi(s,x)}{s(1-h_1^2)\sinh\left(\frac{sL}{c}\right)} & 0 \leqslant x < \xi \leqslant L, \\ G_r(x,\xi;s) = \frac{c\left(\gamma_1(s)\sinh\left(\frac{sx}{c}\right) - \gamma_2(s)\cosh\left(\frac{sx}{c}\right)\right)\varphi(s,\xi)}{s(1-h_1^2)\sinh\left(\frac{sL}{c}\right)} & 0 \leqslant \xi < x \leqslant L. \end{cases} \tag{47}$$

There are two distinctive features in this situation: firstly, the poles of the Green's function are now at $s_n = 0$ and at the values $s_n = \frac{in\pi c}{L}$, $n = \pm 1, 2, \ldots$, and hence the eigenvalues are all imaginary with no real parts!; and, secondly, the pole at zero is a second order pole now. Somewhat surprisingly, we see that damping in the vibratory response therefore disappears now!

Writing the response of the system again as

$$U(x,s) = V_1(x,s) + \frac{a_0}{s} + V_2(x,s) - \frac{1}{c^2}\int_0^x G_r(x,\xi,s)\Gamma(\xi)d\xi - \frac{1}{c^2}\int_x^L G_l(x,\xi,s)\Gamma(\xi,s)d\xi + \frac{a_0}{s} - f(L) \times \frac{h_1}{(1-h_1^2)s\sinh(sL/c)}\varphi(x,s), \tag{48}$$

where

$$\Gamma(x,s) = sf(x) + g(x) + \dot{a}_0 + P(x,s). \tag{49}$$

The inverse Laplace transform of the Green's function (note the double pole at $s = 0$) is given by

$$L^{-1}\{G_{l,r}(x,\xi,s)\} = -\frac{ch_1}{(1-h_1^2)}\left[\frac{x+\xi}{L} - 1\right] - \frac{c^2 t}{(1-h_1^2)L} - \frac{c^2}{(1-h_1^2)L}\sum_{\substack{n=-\infty \\ n\neq 0}}^{\infty}\frac{1}{s_n}\varphi_n(x)\varphi_n(\xi)e^{s_n t} \tag{50}$$

and the inverse transform of $sG_{l,r}(x,\xi,s)$ is given by

$$L^{-1}\{sG_{l,r}(x,\xi,s)\} = -\frac{c^2}{(1-h_1^2)L} - \frac{c^2}{(1-h_1^2)L}\sum_{\substack{n=-\infty \\ n\neq 0}}^{\infty}\varphi_n(x)\varphi_n(\xi)e^{s_n t}, \tag{51}$$

where $s_n = \frac{in\pi c}{L}$, and, as before, $\varphi_n(x) = \cosh\left(\frac{s_n x}{c}\right) + h_1\sinh\left(\frac{s_n x}{c}\right)$. Noting that

$$V_2(x,s) = -f(L)\frac{h_1}{(1-h_1^2)}\frac{\varphi(x,s)}{s\sinh\left(\frac{sL}{c}\right)}, \tag{52}$$

we find that its inverse Laplace transform is

$$L^{-1}\{V_2(x,s)\} = -f(L)h_1\frac{ct+h_1 x}{(1-h_1^2)L} - f(L)\frac{ch_1}{(1-h_1^2)L}\sum_{\substack{n=-\infty \\ n\neq 0}}^{\infty}(-1)^n e^{s_n t}\frac{\varphi_n(x)}{s_n}. \tag{53}$$

Using these relations we obtain the response of the system as

$$\begin{aligned} u(x,t) = {} & a_0 + \frac{1}{(1-h_1^2)L}\int_0^L f(\xi)d\xi - f(L)h_1\frac{ct+h_1 x}{(1-h_1^2)L} - f(L)\frac{ch_1}{(1-h_1^2)L}\sum_{\substack{n=-\infty \\ n\neq 0}}^{\infty}(-1)^n e^{s_n t}\frac{\varphi_n(x)}{s_n} \\ & + \frac{h_1}{c(1-h_1^2)}\left(\frac{x}{L} - 1\right)\int_0^L g(\xi)d\xi + \frac{h_1}{c(1-h_1^2)L}\int_0^L \xi g(\xi)d\xi + \frac{t}{(1-h_1^2)L}\int_0^L g(\xi)d\xi + \dot{a}_0\frac{h_1}{c(1-h_1^2)}\left(x - \frac{L}{2}\right) \\ & + \dot{a}_0\frac{t}{(1-h_1^2)} + \frac{1}{(1-h_1^2)L}\sum_{\substack{n=-\infty \\ n\neq 0}}^{\infty}\varphi_n(x)e^{s_n t}\int_0^L\left[f(\xi) + \frac{\dot{a}_0 + g(\xi)}{s_n}\right]\varphi_n(\xi)d\xi + \frac{h_1}{c(1-h_1^2)}\int_0^t \\ & \times \int_0^L\left[\frac{x+\xi}{L} - 1\right]p(\xi,\tau)d\xi d\tau + \frac{1}{(1-h_1^2)L}\int_0^t (t-\tau)\int_0^L p(\xi,\tau)d\xi d\tau + \frac{1}{(1-h_1^2)L}\sum_{\substack{n=-\infty \\ n\neq 0}}^{\infty}\frac{1}{s_n}\varphi_n(x) \\ & \times \int_0^t e^{s_n(t-\tau)}\left[\int_0^L \varphi_n(\xi)p(\xi,\tau)d\xi\right]d\tau. \end{aligned} \tag{54}$$

One observes that the response of this undamped system is, in general, unbounded. In particular, its response to an initial velocity $\dot{a}_0$ linearly increases with time. Since $q = 0$, one might have intuited that the system would be neutrally stable, but our intuitive thinking is incorrect since the system has a second order pole at zero, which causes its response to become unbounded, and a rigid body motion ensues.

5.3. Response of the system for special values $h_2 = -1/h_1$

As pointed out in Section 3, when $h_2 = -1/h_1$, $q = 0$, and the general expression for the response given in Eq. (39) can be simplified. The Green's function corresponding to the solution $V_1(x,\xi,s)$ becomes

$$G(x,\xi;s) = \begin{cases} G_l(x,\xi;s) = \frac{ch_1\left(\gamma_1(s)\sinh\left(\frac{s\xi}{c}\right) - \gamma_2(s)\cosh\left(\frac{s\xi}{c}\right)\right)\varphi(s,x)}{s(h_1^2-1)\cosh\left(\frac{sL}{c}\right)} & 0 \leqslant x < \xi \leqslant L, \\ G_r(x,\xi;s) = \frac{ch_1\left(\gamma_1(s)\sinh\left(\frac{sx}{c}\right) - \gamma_2(s)\cosh\left(\frac{sx}{c}\right)\right)\varphi(s,\xi)}{s(h_1^2-1)\cosh\left(\frac{sL}{c}\right)} & 0 \leqslant \xi < x \leqslant L, \end{cases} \tag{55}$$

where $\varphi(s,x)$, $\gamma_1(s)$ and $\gamma_2(s)$ are defined in relations (28)–(30). The Green's function now has simple poles at $s = 0$, and at $s_n = \left\{ i\frac{(2n+1)\pi c}{2L} \right\}_{n=-\infty}^{\infty}$. The bar loses all damping.

The inverse Laplace transform of the Green's function then becomes

$$L^{-1}\{G_{l,r}(x,\xi,s)\} = -\frac{ch_1}{(h_1^2-1)} + \frac{c^2}{(h_1^2-1)L}\sum_{n=-\infty}^{\infty}\frac{1}{s_n}e^{s_n t}\varphi_n(x)\varphi_n(\xi) \tag{56}$$

and,

$$L^{-1}\{sG_{l,r}(x,\xi,s)\} = \frac{c^2}{(h^2-1)L}\sum_{n=-\infty}^{\infty}e^{s_n t}\varphi_n(x)\varphi_n(\xi), \tag{57}$$

where as before, $\varphi_n(x) = \cosh(s_n x/c) + h_1 \sinh(s_n x/c)$.

Also, the solution

$$V_2(x,\xi,s) = \frac{f(L)}{s(1-h_1^2)\cosh\left(\frac{sL}{c}\right)}\varphi(x,s), \tag{58}$$

whose inverse Laplace transform is

$$L^{-1}\{V_2(x,\xi,s)\} = \frac{f(L)}{(1-h_1^2)} + f(L)\frac{ch_1}{(1-h_1^2)L}\sum_{n=-\infty}^{\infty} i(-1)^{n+1}e^{s_n t}\frac{\varphi_n(x)}{s_n}. \tag{59}$$

This results in the response

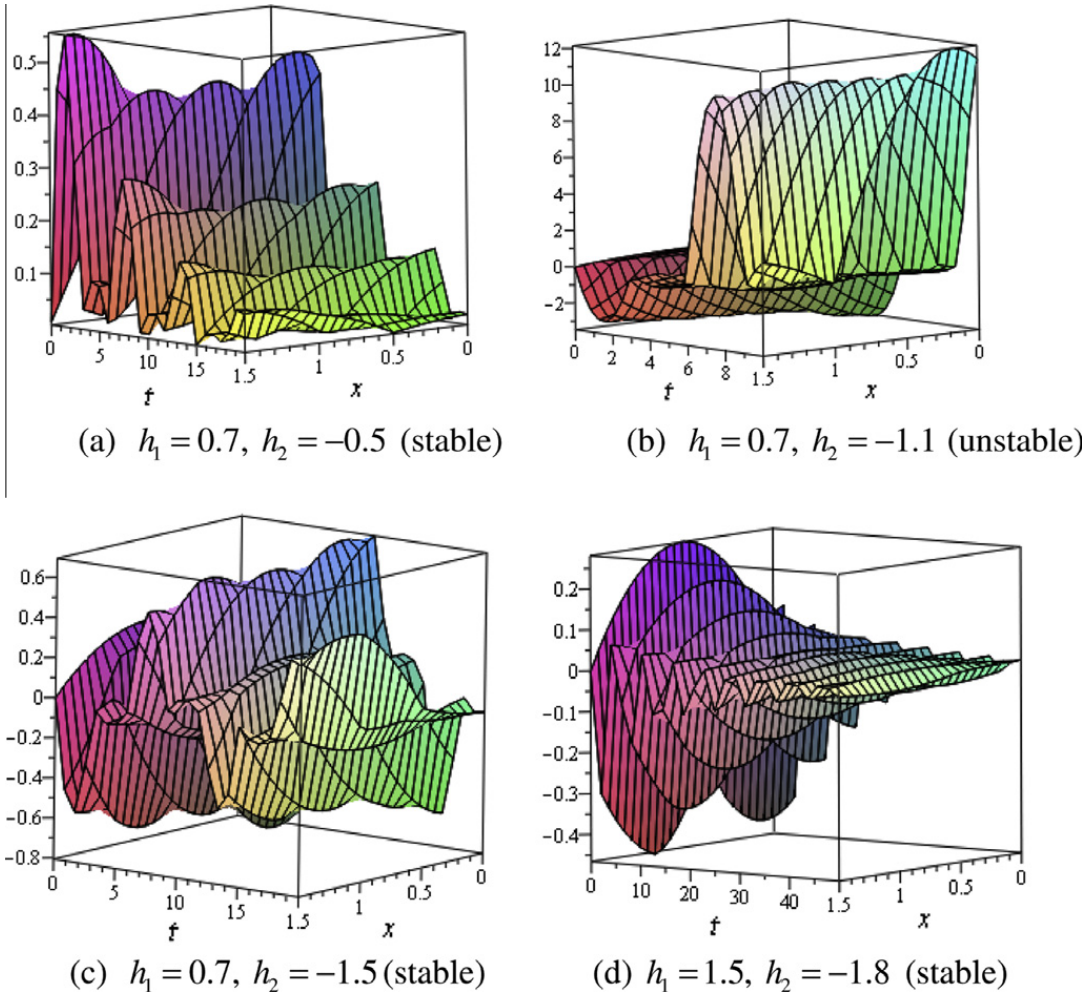

Fig. 7. Response $u(x,t)$ shown on the vertical axis for various combinations of h_1 and h_2. The initial displacement function is $f(x) = x(L-x)$.

$$u(x,t) = \left[a_0 + \dot{a}_0 \frac{h_1 L}{c(h_1^2-1)} + \frac{h_1}{c(h_1^2-1)} \int_0^L g(\xi)d\xi + f(L)\frac{1}{(1-h_1^2)}\right] + \frac{1}{(1-h_1^2)L} \sum_{n=-\infty}^{\infty} \varphi_n(x) e^{s_n t} \int_0^L \varphi_n(\xi)\left[f(\xi) + \frac{g(\xi)+\dot{a}_0}{s_n}\right] d\xi + \frac{h_1}{c(h_1^2-1)} \int_0^t \int_0^L p(\xi,t)d\xi dt + \frac{1}{(1-h_1^2)L} \sum_{n=-\infty}^{\infty} \frac{1}{s_n} \varphi_n(x) \int_0^t e^{s_n(t-\tau)} \left[\int_0^L \varphi_n(x) p(\xi,t) d\xi\right] d\tau + f(L)\frac{ch_1}{(1-h_1^2)L} \sum_{n=-\infty}^{\infty} i(-1)^{n+1} e^{s_n t} \frac{\varphi_n(x)}{s_n}, \quad (60)$$

which could have also been obtained by substituting $h_2 = -1/h_1$ and using the sequence of eigenvalues $s_n = \left\{ i\frac{(2n+1)\pi c}{2L} \right\}_{n=-\infty}^{\infty}$ in Eq. (39).

6. Illustrative examples and computational results

We begin by illustrating the response $u(x,t)$ of the system computed using Eq. (39) for various combinations of the values of h_1 and h_2. All the computations are done using Maple and the analytical expressions obtained were evaluated.

The parameters $c = 0.5$ and $L = 1.5$ are used to describe the characteristics of the bar in all the following computational results; also, the number of terms summed, whenever a series is called for in the analytical solution, is 30.

6.1. General response of the system

We subject the bar only to an initial displacement condition $f(x) = x(L-x)$ to illustrate the somewhat non-intuitive behavior described in Section 3 by taking a value of $h_1 = 0.7$, and showing that stability does not monotonically worsen with

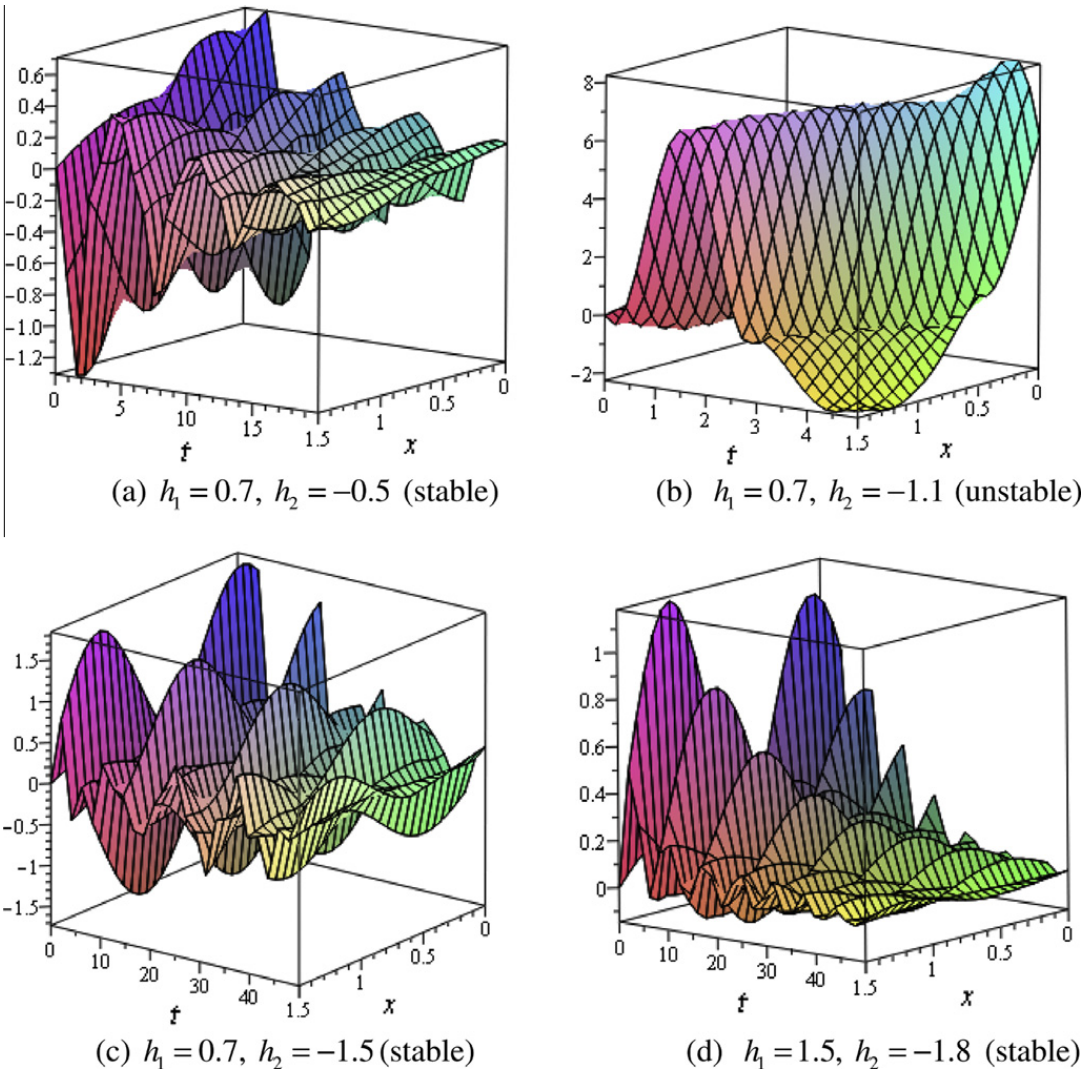

Fig. 8. Response $u(x,t)$ to initial displacement $f(x) = x(L-x)$, and initial velocity $g(x) = \sin(2\pi x/L)$.

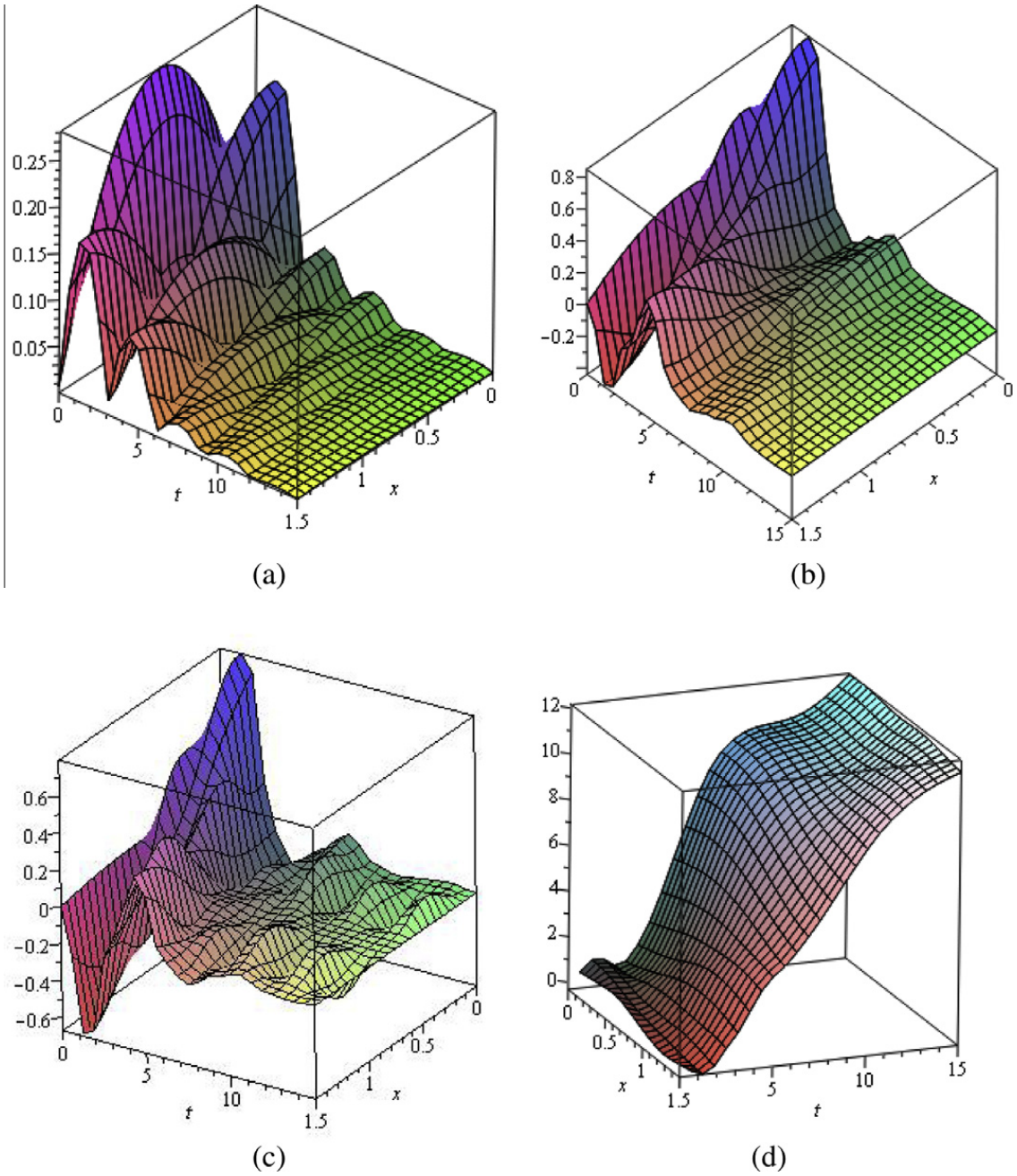

Fig. 9. Response of system with $a_0 = 0$, $h_1 = 0.3$, and $h_2 = 0.6$.

a decrease in the value of h_2. The system is unstable when $h_1 = 0.7$, $h_2 = -1.1$, and regains stability when $h_1 = 0.7$, $h_2 = -1.5$. Furthermore, while $h_1 = 0.7$, $h_2 = -0.5$ is unstable (note, $h_1 > |h_2|$), $h_1 = 1.5$, $h_2 = -1.8$ (note, $h_1 < |h_2|$) is stable!

In Fig. 8 we illustrate the effect of adding to the initial displacement used for Fig. 7 an initial velocity given by $g(x) = \sin(2\pi x/L)$.

The response of the system with $h_1 = 0.3$, $h_2 = 0.6$ is shown in Fig. 9 for:

(a) only an initial displacement $f(x) = x(L - x)$;
(b) only an initial displacement $f(x) = x(L - x)$ and an initial velocity $g(x) = \sin(2\pi x/L)$, with $\dot{a}_0 = -0.05$;
(c) $f(x) = x(L - x)$, $g(x) = \sin(2\pi x/L)$, $\dot{a}_0 = -0.05$, and $p(x,t) = \sin(6\pi x/L)\sin(\pi t/L)$; and,
(d) $f(x) = x(L - x)$, $g(x) = \sin(2\pi x/L)$, $\dot{a}_0 = -0.05$, and $p(x,t) = \sin[(xt)/2]$. These responses are shown in Fig. 9(a)–(d) respectively.

6.2. Super-stability of the bar

Fig. 10(a) shows the response of the system when $h_1 = 0.02$, and $h_2 = 1$, and the bar is excited with an initial displacement $f(x) = x(L - x)/2$ and an initial velocity $g(x) = \sin(2\pi x/L)$, along with $\dot{a}_0 = -0.05$. The response is computed using equation

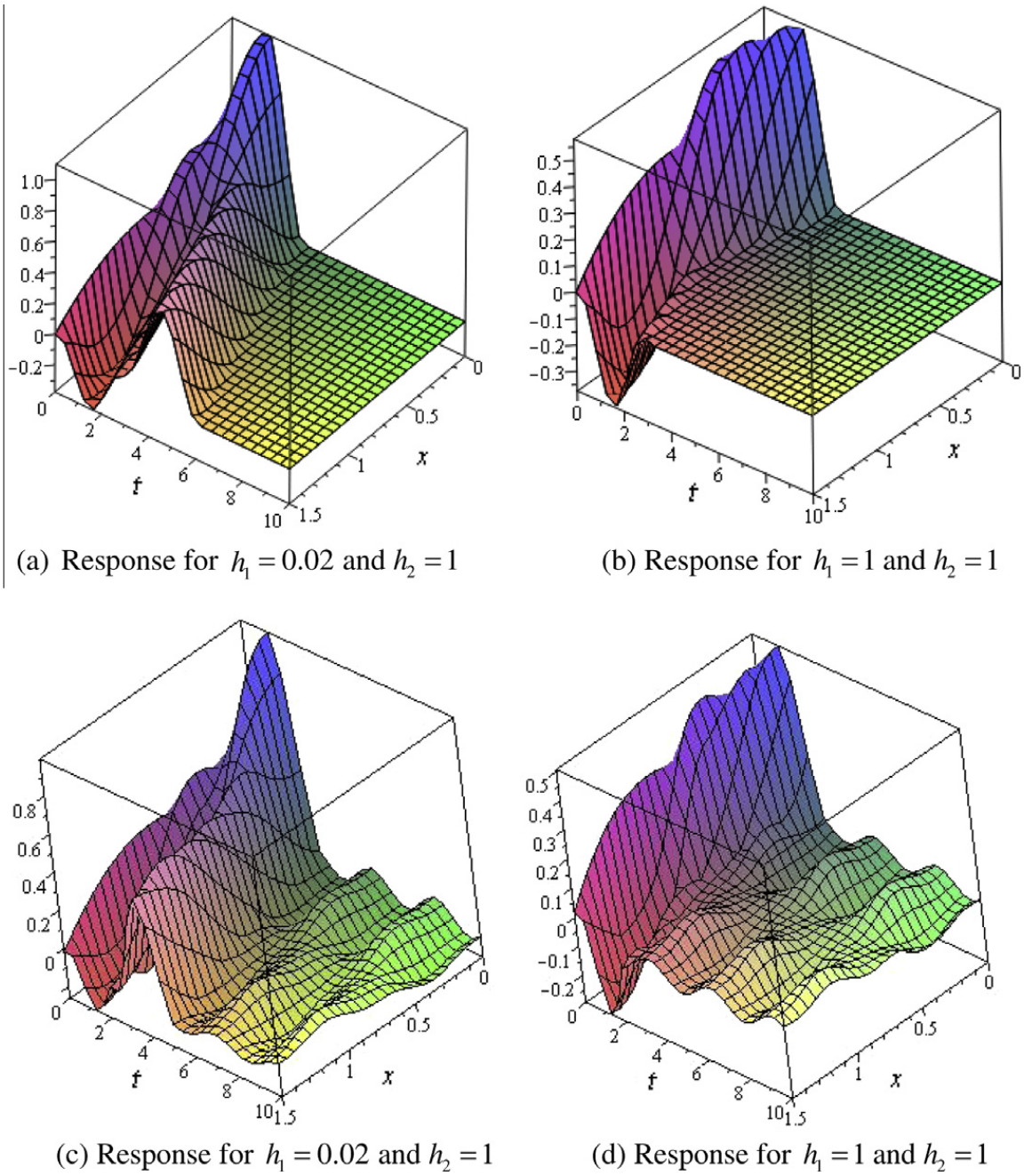

Fig. 10. (a) and (b) show the response to the initial conditions $f(x) = x(L-x)/2$, $g(x) = \sin(2\pi x/L)$, and $\dot{a}_0 = -0.05$. Figures (c) and (d) show the response of the system with the initial conditions $f(x) = x(L-x)/2$, $g(x) = \sin(2\pi x/L)$, and $\dot{a}_0 = -0.05$ and the external excitation $p(x,t) = \sin(6\pi x/L)\sin(\pi t/L)$.

(44). As expected, the response reaches a constant value at $t = 2L/c = 6$ s, illustrating the super-stability of the bar. The response of the same system to the same set of initial conditions is shown in Fig. 10(b), except that now the value of h_1 and h_2 are both taken to be 1. The bar again exhibits super-stability, and comes to rest at the end of $t = L/c = 3$ s as predicted. Fig. 10(c) shows the response of the same system and inputs used in Fig. 10(a), with $h_1 = 0.02$, and $h_2 = 1$, when subjected to the additional external excitation $p(x,t) = \sin(6\pi x/L)\sin(\pi t/L)$. Fig. 10(d) shows the response of the system depicted in Fig. 10(c) to this same additional external excitation but now with $h_1 = 1$, and $h_2 = 1$.

6.3. The Undamped bar

To illustrate the analytical results given in Sub-sections 5.2 and 5.3, Fig. 11(a) shows the response of the system when $h_1 = -1/h_2 \neq 1$, with the value of $h_1 = 0.3$, for the same initial displacement and initial velocity conditions as before, namely $f(x) = x(L-x)/2$, $g(x) = \sin(2\pi x/L)$, and $\dot{a}_0 = -0.05$. We observe that the response has no damping since $q = 0$, and the

eigenvalues are given by $s_n = \{(2n+1)ic\pi/2L\}_{n=-\infty}^{\infty}$. The response of the system with $\dot{a}_0 = -0.05$ when subjected to the external excitation $p(x, t) = \sin(6\pi x/L)\sin(\pi t/L)$ is shown in Fig. 11(b).

Fig. 11(c) and (d) show the response of the system with $h_1 = -h_2 = 0.3$ to the same inputs as those for which Fig. 11(a) and (b) respectively were computed. The system is again undamped and the eigenvalues are $s_n = \{inc\pi/L\}_{n=-\infty}^{\infty}$. Fig. 11(d) shows that as the bar is being driven by the external excitation $p(x,t) = \sin(6\pi x/L)\sin(\pi t/L)$.

7. Quiet boundaries, eigenvalues and impedance matching

In Section 5.1 we observed that when $h_2 = 1$ with $h_2 \neq -1$, the solution of to the motion of the bar contains no eigenfunctions and shows no mode shapes of vibration. Here we explain this somewhat curious behavior and point out that this circumstance is a result of impedance matching between the bar and the damper at the right hand end (Berkhovskikh & Goncharov, 1984). Such matching results in so-called 'quiet boundaries' across which waves in the bar move without any hinderences and reflections. For simplicity we temporarily take in this section the x coordinate to be zero at the right boundary (see Fig. 12).

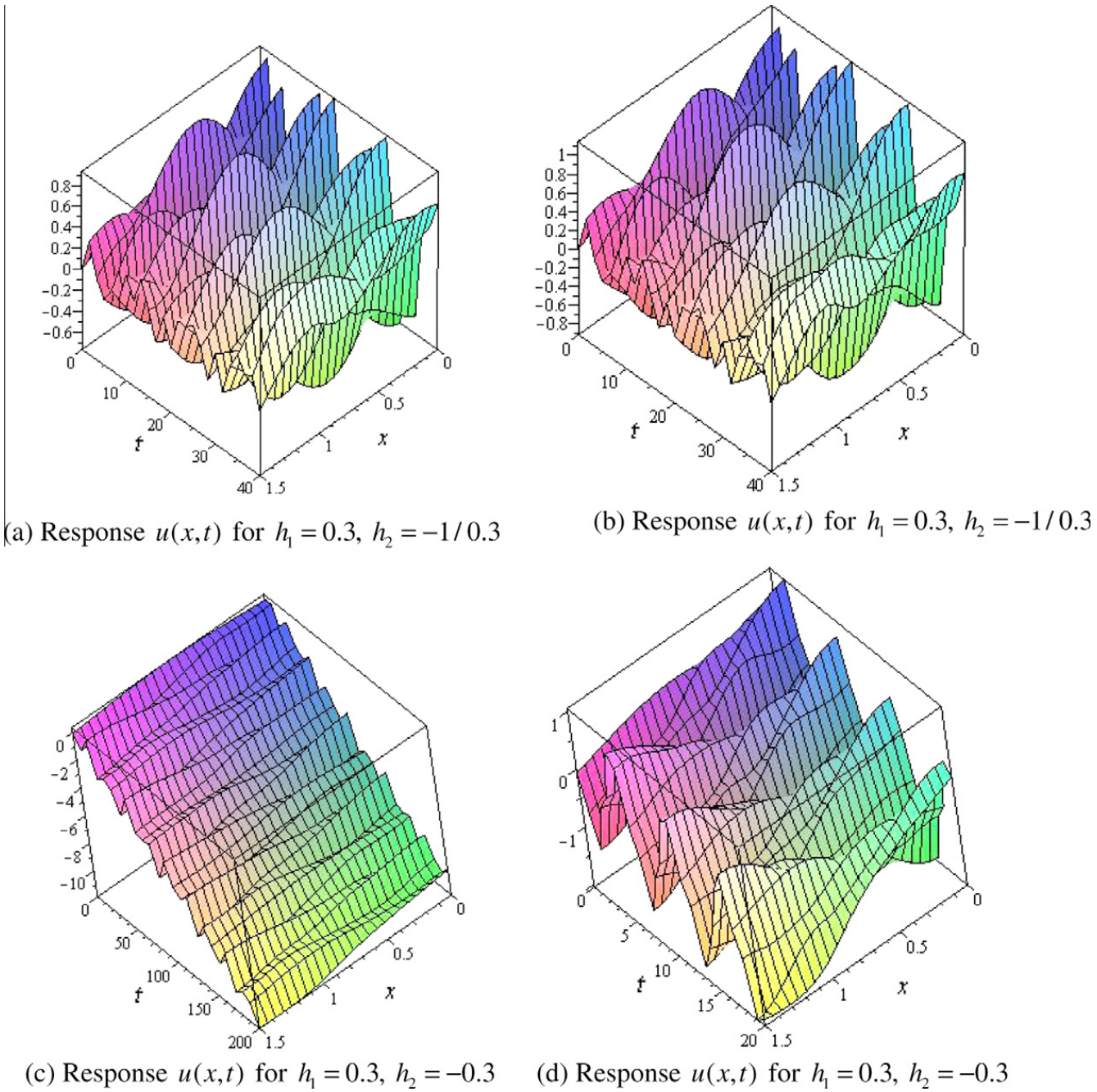

Fig. 11. Response of the undamped system. Figures (a) and (b) are for the system when $h_1 = -1/h_2$. Figures (c) and (d) shows the rigid-body response of the system superposed on its vibratory response when $h_1 = -h_2$.

Considering the incident and reflected waves from the boundary $x = 0$ as

$$v_r(x,t) = Ae^{ik(x-ct)} + AR_r e^{-ik(x+ct)}, \tag{61}$$

they must satisfy the boundary condition on the right

$$\frac{\partial}{\partial x} v_r(0,t) = -\frac{h_2}{c}\frac{\partial}{\partial t} v_r(0,t), \tag{62}$$

which yields the reflection coefficient at the right boundary

$$R_r = \frac{1-h_2}{1+h_2}. \tag{63}$$

Analogously, if the incident and reflected waves are traveling towards and away from the left boundary we have the reflection coefficient

$$R_l = \frac{1-h_1}{1+h_1}, \tag{64}$$

which is exactly what we had defined as η_1 previously. We obtained this terms earlier by determining the inverse Laplace transform in the case dealt with in Section 5.1.

Consider now $v(x,t) = Ae^{ik(x-ct)}$ traveling towards the right boundary with no reflection from the boundary. For such a motion, the force at the right boundary is $F(0,t) = EA_0 \frac{\partial v(0,t)}{\partial x} = iEA_0 k e^{ki(x-ct)}$, while $v(0,t) = -ikcAe^{ki(x-ct)}$. The impedance of the bar, Z_b, to the incoming wave, by definition, is given as

$$Z_b = -\frac{F(0,t)}{\frac{\partial v(0,t)}{\partial t}} = \frac{EA_0}{c}. \tag{65}$$

On the other hand if a dashpot j is acted upon by a force $F_j(t)$ its impedance, Z_d, is

$$Z_{d_j} = \frac{F_j(t)}{\frac{dv_j(t)}{dt}} = c_j. \tag{66}$$

Both these impedances are real and from our definition $h_j = \frac{c_j c}{EA}$ we see that $h_j = \frac{Z_{d_j}}{Z_b}$, $j = 1, 2$. Therefore, the reflection coefficients can be written as $R_l = \frac{Z_b - Z_{d_1}}{Z_b + Z_{d_1}}$ and $R_r = \frac{Z_b - Z_{d_2}}{Z_b + Z_{d_2}}$. When $Z_b = Z_{d_j}$ the impedances 'match,' and $h_j = 1$; dashpot j then acts as a perfect absorber making the corresponding coefficient of reflection zero. We also see that the reflection coefficients are independent of frequency and hold for waves of all frequencies.

We now make several observations with regards to the reflection coefficients obtained above when $h_1, h_2 > 0$.

7.1. Observations

1. When $h_1 \neq 1$ and $h_2 = 1$, the corresponding reflection coefficient at the right hand end is zero. The boundary behaves as if it were not there since it does not modify the incoming wave and it can be called a quiet boundary. The bar 'appears' like a semi-infinite (or infinite) bar since the wave 'disappears' past the right hand boundary as if it were going along an infinite medium. For any initial displacement $f(x)$ the waves reflect at most once from the left hand end of the bar (see Fig. 13), since the right travelling waves 'see' no boundary. The maximum time for that to happen is $2L/c$, and hence in the absence of external excitation after this time every point of the bar comes to rest.
2. The response of the system can be described as fundamentally governed by operator $L_{x,t} = \frac{\partial^2}{\partial t^2} - c^2 \frac{\partial^2}{\partial x^2}$ valid throughout the domain $(0,L)$. The 'boundary conditions' serve to modify the response caused by this operator. For various values of parameters h_1 and h_2 in the boundary they may cause reflections of the waves. This may lead to interference patterns and standing waves that are associated with mode shapes and frequencies of vibrations.
3. When $h_1 = 1$ and/or $h_2 = 1$ the right and/or left boundary generates no reflections, no interference patterns, no standing waves, and hence the response of the system cannot be expressed in terms of eigenvalues or eigenfunctions. All the poles of the Green's function, except for the pole at $s = 0$, are in the extreme left half of the s-plane and have real parts $-\infty$. Energy is irretrievably 'leaked' out of the system because the traveling waves simply disappear past the boundaries and nothing is reflected back. The waves continue onwards as if the boundaries were completely 'transparent' to them. The boundaries act as a 'sink' of energy and drain the energy out of the vibrating system.

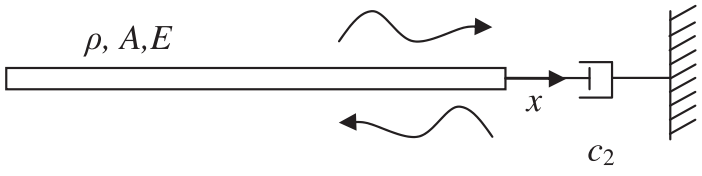

Fig. 12. Incident and reflected wave propagating toward and away from the right boundary of the bar.

4. For $h_1 \neq 1$ and/or $h_2 \neq 1$ this transparency is lost. There are continuing reflections from the boundaries. Reflection coefficients also give us a way to find decay/amplification of waves in the bar. Assume a displacement impulse with amplitude A originating at some point x on the bar and zero initial displacement and $h_i < 1$. After the time of initial impulse there are two waves with amplitude $\frac{A}{2}$ each traveling left and right. After the reflection occurs, the amplitude of the left reflected wave becomes $\frac{R_l A}{2}$ while the amplitude of the right reflected wave becomes $\frac{R_r A}{2}$. Each reflected wave will continue on its journey to the opposite boundary and will be getting altered by the coefficient of reflection at that boundary. When the left reflected wave arrives to the right boundary its amplitude will change to $\frac{R_l A}{2} R_r$, and when the right reflected wave arrives to the left boundary its amplitude will change to $\frac{R_r A}{2} R_l$, and so on. As the two waves pass each other every $\frac{L}{c}$ seconds at locations x or $L–x$ they will be added to give the total amplitude of motion at the locations at which they cross. Therefore, the total amplitude at times $t_n = \frac{nL}{c}$ will be

$$A_n = \begin{cases} A(R_l R_r)^{\frac{n}{2}} & n = 0, 2, 4, \ldots, \\ A(R_l R_r)^{\frac{n-1}{2}} \left(\frac{R_l + R_r}{2}\right) & n = 1, 3, 5 \ldots \end{cases} \tag{67}$$

When $h_1 = h_2$ both reflection coefficients are the same $R = R_l = R_r$ and the amplitude is simply $A_n = A\,R^n$ at times $t_n = \frac{nL}{c}$ for $n = 0, 1, 2, 3, \ldots$ In this case the amplitudes are bounded by the curve $AR^{\frac{ct}{L}}$. The factor $R^{\frac{ct}{L}}$ is indeed just the real part of $e^{s_n t}$ where s_n is given by Eq. (9), since $e^{\frac{cq}{2L}t} = e^{\frac{ct}{L}\ln R} = R^{\frac{ct}{L}}$.

5. Assuming that $0 \leqslant h_1 < 1$, $h_2 = 1$ and that the bar starts with zero initial velocity under no external excitation with the displacement pulse shown in Fig. 13, changes of its total energy $E(t)$ with time are shown in Fig. 14. Starting with a total energy E_0, the energy remains constant until the right traveling wave disappears at the right boundary. The energy then drops by half at time $(L - x_0)/c$. After this the energy remains constant for a duration of time while the leftward traveling wave moves towards the left boundary. At the left boundary the wave is reflected and proceeds towards the right boundary. At that time the energy drops to $\left(\frac{1-h_1}{1+h_1}\right)^2 \frac{1}{2} E_0$ and remains constant until this reflected wave disappears past the right boundary as well. We observe from Fig. 14 that the $\dot{E}(t)$ is zero for a considerable length of time. Hence, asymptotic stability cannot be directly deduced from Lyapunov's theorem by using $E(t)$ as a Lyapunov function. In fact we have a much stronger result here: the response goes to zero, not exponentially in time, but after a time $\frac{2L}{c}$ which is finite.

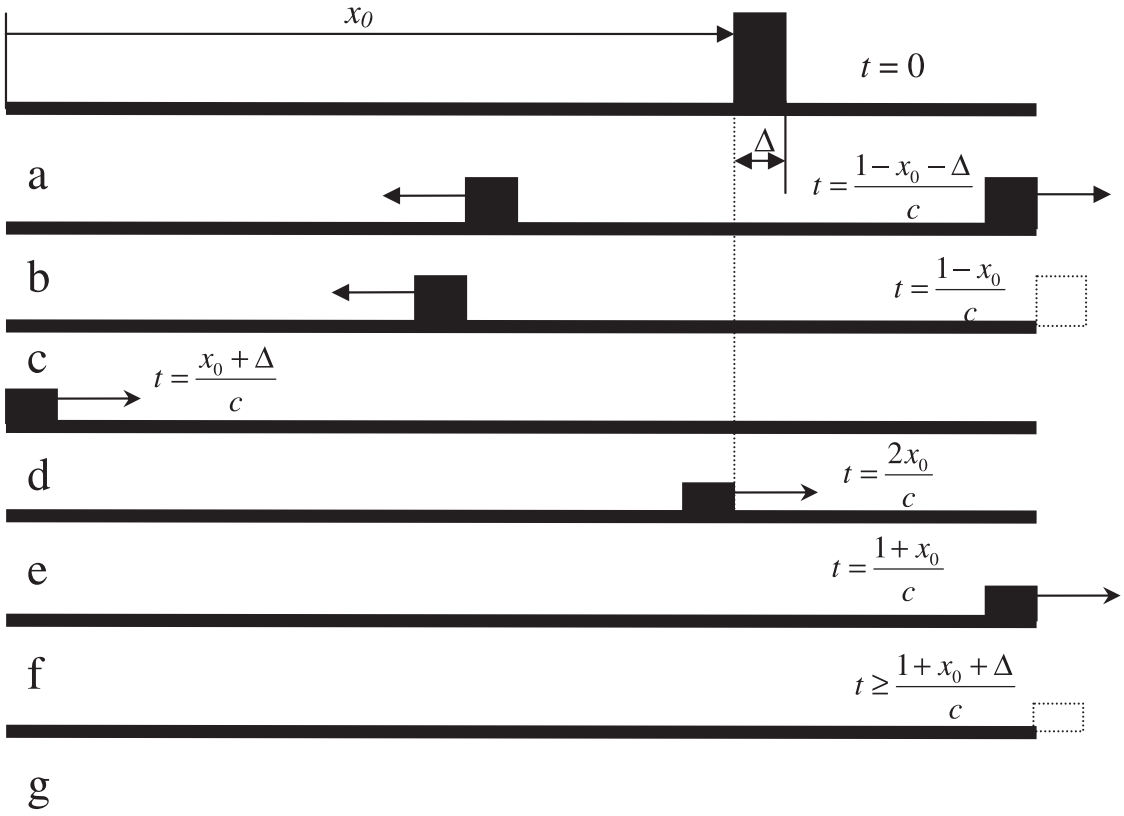

Fig. 13. The vibratory response at successive times due to an initial displacement pulse for $0 \leqslant h_1 < 1$, $h_2 = 1$. (a) The displacement response initially splits in two, each half moving in the opposite directions. (b) The right moving half 'disappears' beyond the right end of the bar. (c) The left wave is then reflected and travels (d) towards the right boundary (e). (f) Eventually this wave disappears as well and the bar is et rest (g).

When $h_1 = -1$ or $h_2 = -1$, the corresponding reflection coefficients become infinite which means that the total wave reaches an infinite amplitude upon reflection. Therefore, an infinite response amplitude is reached in finite time to an initial displacement – the system is 'super-unstable'. There is thus a similarity of behavior of our system with that of so-called 'finite exit-time' of some nonlinear systems, except that our system is described by a linear partial differential equation with constant coefficients.

8. Discretization

In this section we explore discretization of the continuous bar and show some interesting consequences. Applying any finite difference or finite element scheme to Eqs. (1)–(3) achieves such a discretization of the system and provides a linear system of equations with constant coefficients. To expose the essence of our discussion we will concentrate in this section on the situation in which the bar is subjected to no external excitation. Discretization would then lead to a set of linear ordinary differential equations

$$\frac{du}{dt} = Au, \quad u(t=0) = u_0 \tag{68}$$

were A is a constant N by N square matrix where N is the number of mesh points chosen to discretize the spatial domain $(0,L)$. Eq. (68) represents a finite-dimensional system of the first order ordinary differential equations that can be easily solved. To understand this approximation scheme, we solve for the poles of the system in the s-plane.

$$\det(A - sI) = 0. \tag{69}$$

By the fundamental theorem of algebra, we must obtain N finite roots of the Nth order polynomial in Eq. (69). However, we found earlier that for $h_2 = 1$ and $h_1 \neq -1$ or $h_1 = 1$ and $h_2 \neq -1$ all the poles of the continuous system are at infinity, save the pole at the origin, i.e. all but one pole are in the left half of s-plane with their abscissas at $-\infty$. Hence it is impossible to obtain a qualitatively correct approximation of the continuous system when $h_2 = 1$ and $h_1 \neq -1$ or $h_1 = 1$ and $h_2 \neq -1$ *regardless of how large N* is taken to be. We can state this alternatively. When $h_2 = 1$ and $h_1 \neq -1$ or $h_1 = 1$ and $h_2 \neq -1$ the continuous system has no finite poles, except for the one at $s = 0$. *Therefore, it is impossible for any finite dimensional scheme to qualitatively approximate the behavior of the bar* for these parameter values.

Moreover, the general solution of Eq. (68) is

$$u(t) = e^{At}u_0. \tag{70}$$

Since no general exponential solution can go to zero in finite time, the discretized equations cannot cause the response to go to zero (or to become infinite) in finite time. Therefore, the super-stable behavior of our continuous system that comes to a 'dead stop' when (for $h_2 = 1$ and $h_1 \neq -1$ or $h_1 = 1$ and $h_2 \neq -1$) after time $\frac{2L}{c}$ can never be qualitatively mimicked by any

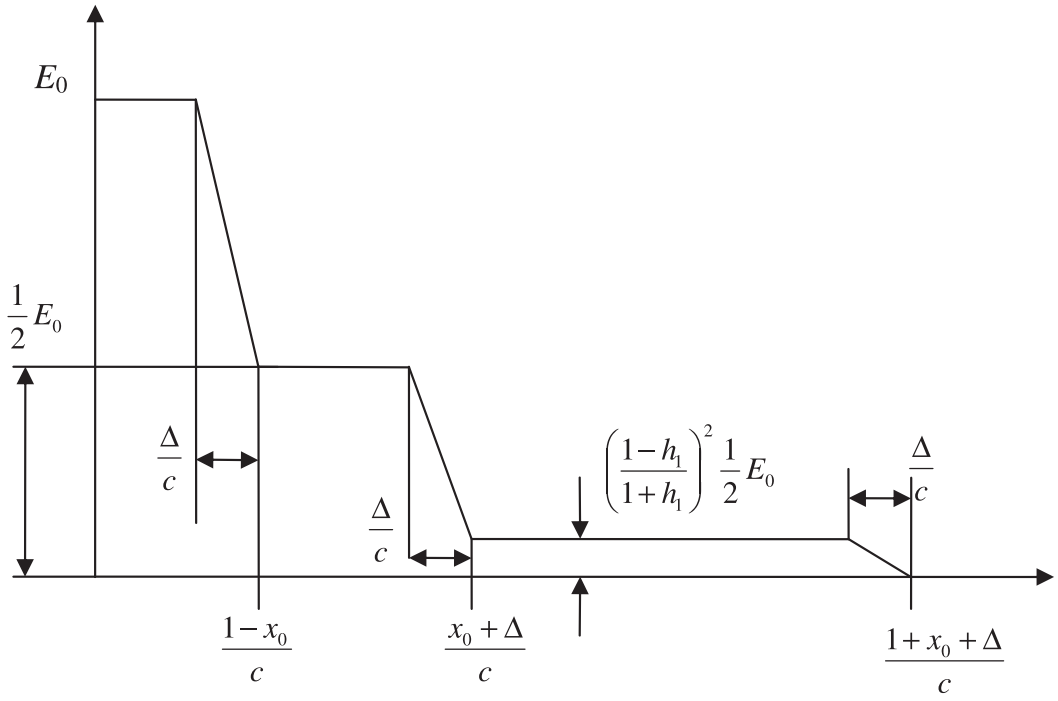

Fig. 14. A schematic plot of total energy versus time for the displacement pulse shown in Fig. 13.

discrete approximation scheme, regardless of how finely we discretize the spatial domain. This super-stable behavior is a consequence of the continuum nature of our system; it qualitatively disappears as soon as any finite dimensional approximation of the continuum is made.

A similar argument can be made for super-unstable behavior which causes the response of the system to become unbounded in finite time when $h_1 = -1$ or $h_2 = -1$. However, no system described by the constant coefficient set of linear ordinary differential equations given in Eq. (68) can have an unbounded response in finite time. This super-unstable behavior too is a consequence of the continuum nature of the partial differential equation model described in Eq. (1) and it cannot be qualitatively captured regardless of how large we take N to be.

9. Conclusions

This paper studies the dynamics of the longitudinal vibrations of a bar subjected to viscously controlled boundaries on each end. The system is not self-adjoint, and closed form expressions for the general response of the system to arbitrary initial conditions and external excitation are obtained using Green's functions. Though seemingly commonplace, the system exhibits non-intuitive behavior when the boundary feedback parameters h_1 and h_2 are varied. In particular, three interesting phenomena are discussed: super-instability, super-stability, and loss of damping. The first causes the response of the system to become unbounded in finite time, the second causes the system to come to rest in finite time. These types of behavior can occur in nonlinear systems, but are extremely rare in linear systems. In this case their presence, it appears, is intricately related to the continuum modeling of the system. We show that the third phenomenon – loss of damping – is a situation that can be created in the bar with appropriate boundary feedback control, and has practical implications for the creating undamped systems through boundary feedback. Thus, the behavior of the system has several interesting characteristics. The main contributions of this paper are the following.

1. The stability of the system is investigated for various parameter values that describe the feedback boundary control force. We show that the stability characteristics of the system are complex in the $h_1 - h_2$ plane. Numerical verification of the non-intuitive behavior of the response of this system is provided by computational results.
2. Closed form results are provided for the system in various regions of the parameter space. These closed form solutions show the non-intuitive behavior of the system in these parameter regimes.
3. We show that the behavior of the system depends on the value of the parameters h_1 and h_2 that give the magnitude of the boundary feedback force. In the absence of external excitation, when $h_1 = 1$ or $h_2 = 1$, the bar comes to rest in finite time. We explain the presence of such behavior which has been referred to as super-stable (Balakrishnan, 2002; Udwadia, 2005).
4. We show that the boundary feed back parameters can be adjusted so that the bar's vibratory motion becomes completely undamped. This occurs when $h_1 = -h_2$ and when $h_1 h_2 = -1$. While both cases exhibit no damping the eigenfrequencies are different for the two cases.
5. Super-stable behavior is explained via the analysis of traveling waves propagating across the medium that produce no reflections at the right-hand and/or left-hand boundaries. This leads to the disappearance of eigenvalues and eigenfunctions, except for the one corresponding to the pole at the origin. In this case the Green's function has all its poles, save the one at $s = 0$, in the extreme left half complex plane with their abscissas all at $-\infty$. From a physical standpoint, we show that this happens when there is a match of impedances of the dashpot(s) and the bar.
6. The analysis also shows the presence of super-unstable behavior when $h_1 = -1$ and $h_2 = -1$. The response of the system becomes infinite in finite time. However, the system has no eigenvalues and eigenfunctions, except for the one corresponding to the pole at the origin. Every pole of the Green's function of the system is now at the extreme right hand end of the complex plane and has an abscissa at $+\infty$, except for the pole at $s = 0$.
7. Most importantly, this paper demonstrates that no finite dimensional model obtained through spatial discretization, *regardless of how fine this discretization be*, can qualitatively capture the super-unstable and super-stable behavior of the continuous system. These properties appear to be intrinsic to the continuum nature of the model and cannot be qualitatively obtained from any finite dimensional approximations of the continuum.

Most computational methods assume that the response obtained by discretizing a system qualitatively approaches that of the continuous system as the discretization is made finer and finer (say, for example, by using more and more finite elements). However, from a mathematical view point, one might imagine that there might be situations where this assumption may not be valid since the countable infinity with cardinality $\aleph_0$ generated through such discretizations is nowhere near the $\aleph_1$ cardinality of the continuum. The super-stable (unstable) response of the bar appears to be one such situation where this difference in cardinalities (there are apparently no sets with cardinalities between these two) of the two sets manifests itself significantly. It causes the response of the bar obtained from any finite sized discretization, no matter how fine, to be qualitatively different from that of the continuum.

The governing equations that we have used to describe the system arise in numerous fields like structural dynamics, structural control, acoustics, earthquake engineering, and computational mechanics, and we hope that the results obtained

in this paper will shed light in these and other application areas. The analytical results obtained in this paper do not appear to have been reported in the literature to date.

Appendix A

A.1

The Green's function can be obtained as follows.

The general solution to homogeneous equation for $V_1(x,s)$ that satisfies the boundary condition at the left hand end ($x = 0$) is

$$v_l(x,s) = A\left[\cosh\left(\frac{sx}{c}\right) + h_1 \sinh\left(\frac{sx}{c}\right)\right].$$

Similarly, a solution that satisfies the right hand boundary condition at $x = L$ is

$$v_r(x,s) = B\left[\cosh\left(\frac{s(L-x)}{L}\right) + h_1 \sinh\left(\frac{s(L-x)}{L}\right)\right].$$

In order to ensure continuity of the Green's function at $x = \xi$ we thus consider the function

$$G_l(x,\xi,s) = A\left[\cosh\left(\frac{sx}{L}\right) + h_1 \sinh\left(\frac{sx}{L}\right)\right]\left[\cosh\left(\frac{s(L-\xi)}{L}\right) + h_1 \sinh\left(\frac{s(L-\xi)}{L}\right)\right], \text{ for } 0 \leqslant x < \xi \leqslant L$$

$$G_r(x,\xi,s) = A\left[\cosh\left(\frac{s\xi}{L}\right) + h_1 \sinh\left(\frac{sx}{L}\right)\right]\left[\cosh\left(\frac{s(L-x)}{L}\right) + h_1 \sinh\left(\frac{s(L-x)}{L}\right)\right], \text{ for } 0 \leqslant \xi < x \leqslant L.$$

Enforcing the jump condition on the derivative at $x = \xi$ we obtain

$$A = -\frac{c}{s[\gamma_1(s) + h_1\gamma_2(s)]}.$$

Noting that

$$\cosh\left(\frac{s(L-x)}{L}\right) + h_1 \sinh\left(\frac{s(L-x)}{L}\right) = \gamma_2(s)\cosh\left(\frac{sx}{L}\right) - \gamma_1(s)\sinh\left(\frac{sx}{L}\right).$$

The result given in Eq. (27) follows.

In a similar manner the Green's functions given in Eqs. (41), (47) and (55) can be found.

A.2

The solution to the homogeneous boundary value problem for $V_2(x,s)$ can be assumed to be

$$V_2(x,s) = A\cosh\left(\frac{sx}{c}\right) + B\sinh\left(\frac{sx}{c}\right).$$

Using the boundary condition at the end $x = 0$ we get $B = h_1 A$, so that

$$V_2(x,s) = A\left[\cosh\left(\frac{sx}{c}\right) + h_1 \sinh\left(\frac{sx}{c}\right)\right].$$

The boundary condition

$$\frac{dV_2(L,s)}{dx} = -h_2\frac{s}{c}V_2(L,s) + f(L)\frac{h_2}{c},$$

then yields

$$A = f(L)\frac{h_2}{s[\gamma_1(s) + h_1\gamma_2(s)]}.$$

From which relation (33) follows.

Similarly, the solutions for $V_2(x,s)$ in Eqs. (52) and (58) can be found.

A.3

The inverse Laplace transform can be found by integrating in a closed contour that encloses all the poles of the system.

$$L^{-1}[G_l(x,\xi,s)] = \frac{1}{2\pi i}\oint \frac{c(\sinh\left(\frac{s\xi}{c}\right)\gamma_1(s) - \cosh\left(\frac{s\xi}{c}\right)\gamma_2(s))\varphi(x,s)e^{st}}{s[\gamma_1(s) + h_1\gamma_2(s)]}ds,$$

where we have defined the various quantities in Eqs. (28)–(31). We have simple poles at $s = 0$ and $\gamma_1(s_n) + h_1\gamma_2(s_n) = 0$.

Since $\lim_{s\to 0}\gamma_1(s) = h_2$, $\lim_{s\to 0}\ \gamma_2(s) = 1$, $\lim_{s\to 0}\varphi(x,s) = 1$, the residue at the pole $s = 0$ is simply $-\frac{c}{(h_1+h_2)}$, provided $h_1 + h_2 \neq 0$.

For the residues at the poles $s = s_n$, we first note that $\frac{d\gamma_{1,2}}{ds} = \frac{L}{c}\gamma_{2,1}$, and that $\gamma_1(s_n) = -h_1\gamma_2(s_n) = 0$. The residue at $s = s_n$ then becomes

$$\frac{c^2\left(\sinh\left(\frac{s_n\xi}{c}\right)\gamma_1(s_n) - \cosh\left(\frac{s_n\xi}{c}\right)\gamma_2(s_n)\right)\varphi(x,s_n)e^{s_nt}}{Ls_n\left[\frac{d\gamma_1(s_n)}{ds} + h_1\frac{d\gamma_2(s_n)}{ds}\right]} = \frac{c^2\left(-h_1\sinh\left(\frac{s_n\xi}{c}\right) - \cosh\left(\frac{s_n\xi}{c}\right)\right)\gamma_2(s_n)\varphi(x,s_n)e^{s_nt}}{Ls_n[\gamma_2(s_n) + h_1\gamma_1(s_n)]}$$

$$= \frac{c^2\left(-h_1\sinh\left(\frac{s_n\xi}{c}\right) - \cosh\left(\frac{s_n\xi}{c}\right)\right)\varphi(x,s_n)e^{s_nt}}{Ls_n(1-h_1^2)},$$

provided $\gamma_2(s_n) \neq 0$ and $h_1 \neq 1$. The last expression can be rewritten as

$$-\frac{c^2\varphi(\xi,s_n)\varphi(x,s_n)e^{s_nt}}{s_nL[1-h_1^2]} = -\frac{c^2\varphi_n(\xi)\varphi_n(x)e^{s_nt}}{s_nL[1-h_1^2]},$$

where $\varphi_n(\xi) = \cosh\left(\frac{s_n\xi}{c}\right) + h_1\sinh\left(\frac{s_n\xi}{c}\right)$. Hence,

$$L^{-1}[G_l(x,\xi,s)] = -\frac{c}{(h_1+h_2)} - \frac{c^2}{(1-h_1^2)L}\sum_{n=-\infty}^{\infty}\frac{1}{s_n}e^{s_nt}\varphi_n(\xi)\varphi_n(x).$$

Similarly, $L^{-1}[sG_l(x,\xi,s)]$ can be found observing that $sG_l(x,\xi,s)$ has only simple poles at $\gamma_1(s_n) + h_1\gamma_2(s_n) = 0$.

We can expand the Green's function in Eqs. (47) and (55) in a similar manner.

A.4

$$L^{-1}[V_2(x,s)] = L^{-1}\left[f(L)\frac{h_2}{s\Delta(s)}\varphi(x,s)\right] = \frac{1}{2\pi i}\oint f(L)\frac{h_2}{s\Delta(s)}\varphi(x,s)e^{st}ds,$$

where the contour encompasses all the poles. The residues at the pole $s = 0$ is then given by

$$f(L)\frac{h_2}{s\Delta(s)}\varphi(x,s)e^{st} = f(L)\lim_{s\to 0}\frac{h_2\varphi(x,s)e^{st}}{[\gamma_1(s) + h_1\gamma_2(s)]} = f(L)\frac{h_2}{h_1+h_2},\ h_1 + h_2 \neq 0.$$

The residue at the poles given by $\gamma_1(s_n) + h_1\gamma_2(s_n) = 0$, is obtained as

$$f(L)\frac{h_2\varphi(x,s_n)e^{s_nt}}{\left[\frac{d\gamma_1(s_n)}{ds} + h_1\frac{d\gamma_2(s_n)}{ds}\right]} = f(L)\frac{h_2c\varphi(x,s_n)e^{s_nt}}{L[\gamma_2(s_n) + h_1\gamma_1(s_n)]} = f(L)\frac{h_2c}{(1-h_1^2)L}e^{s_nt}\frac{\varphi_n(x)}{\gamma_2(s_n)}$$

and hence, we obtain

$$L^{-1}\left[f(L)\frac{h_2}{s\Delta(s)}\varphi(x,s)\right] = f(L)\frac{h_2}{h_1+h_2} + f(L)\frac{h_2c}{(1-h_1^2)L}\sum_{n=-\infty}^{\infty}\frac{\varphi_n(x)e^{s_nt}}{s_n\gamma_2(s_n)}.$$

We can similarly expand $L^{-1}[V_2(x,s)]$ to obtain Eqs. (53) and (59).

References

Balakrishnan, A. V. (2002). Superstability: Theory and experiment. In *12th international workshop on dynamics and control, August 19–21*.

Barclay, A., Gill, P. E., & Rosen, J. B. (1998). SQP methods and their applications to numerical optimal control. In W. H. Schmidt, K. Heier, L. Bittner, & R. Bulirsch (Eds.), *Variational calculus, optimal control and applications. International Series of Numerical Mathematics* (Vol. 124, pp. 207–222). Basel: Birkhäuser.

Berkhovskikh, L., & Goncharov, V. (1984). *Mechanics of continua and wave dynamics*. Springer Verlag.

Gürgöze, M., & Erol, H. (2006). Dynamic response of a viscously damped cantilever with a viscous end condition. *Journal of Sound and Vibration, 298*, 132–153.

Hull, A. J. (1994). A closed form solution of a longitudinal bar with a viscous boundary condition. *Journal of Sound and Vibration, 169*(1).

Lions, J. L. (1971). *Optimal control of systems governed by partial differential equations*. Springer-Verlag.

Lions, J. L. (1988). Exact controllability, stabilization and perturbations for distributed systems. *SIAM Review, 30*.

Udwadia, F. E. (2005). Boundary control, quiet boundaries, super-stability and super-instability. *Applied Mathematics and Computation, 164*, 327–349.